Braz J Phys (2012) 42:487–504
DOI 10.1007/s13538-012-0087-9

GENERAL AND APPLIED PHYSICS

Effect of Temperature Anisotropy on Various Modes and Instabilities for a Magnetized Non-relativistic Bi-Maxwellian Plasma

Muhammad Fraz Bashir · G. Murtaza

Received: 29 September 2011 / Published online: 3 July 2012

Abstract Using kinetic theory for homogeneous collisionless magnetized plasmas, we present an extended review of the plasma waves and instabilities and discuss the anisotropic response of generalized relativistic dielectric tensor and Onsager symmetry properties for arbitrary distribution functions. In general, we observe that for such plasmas only those modes whose magnetic-field perturbations are perpendicular to the ambient magnetic field, i.e., $\mathbf{B}_1 \perp \mathbf{B}_0$, are effected by the anisotropy. However, in oblique propagation all modes do show such anisotropic effects. Considering the non-relativistic bi-Maxwellian distribution and studying the relevant components of the general dielectric tensor under appropriate conditions, we derive the dispersion relations for various modes and instabilities. We show that only the electromagnetic R- and L- waves, those derived from them (i.e., the whistler mode, pure Alfvén mode, firehose instability, and whistler instability), and the O-mode are affected by thermal anisotropies, since they satisfy the required condition $\mathbf{B}_1 \perp \mathbf{B}_0$. By contrast, the perpendicularly propagating X-mode and the modes derived from it (the pure transverse X-mode and Bernstein mode) show no such effect. In general, we note that the thermal anisotropy modifies the parallel propagating modes via the parallel acoustic effect, while it modifies the perpendicular propagating modes via the Larmor-radius effect. In oblique propagation for kinetic Alfvén waves, the thermal anisotropy affects the kinetic regime more than it affects the inertial regime. The generalized fast mode exhibits two distinct acoustic effects, one in the direction parallel to the ambient magnetic field and the other in the direction perpendicular to it. In the fast-mode instability, the magneto-sonic wave causes suppression of the firehose instability. We discuss all these propagation characteristics and present graphic illustrations. The threshold conditions for different instabilities are also obtained.

Keywords Plasma waves and instabilities · Temperature anisotropy · Relativistic plasma · Nonrelativistic plasma · Homogeneous and magnetized plasmas · R- and L- waves · Whistler wave and instability · Aflvén wave · Firehose instability · X-mode · O-mode · Bernstein wave · Kinetic Alfvén Waves · Inertial Alfvén wave · Fast mode and fast mode instability

1 Introduction

Extensive studies have been conducted over the years using a wide variety of particle distributions to derive the general dielectric tensor so as to study various modes and instabilities [1–11]. Brambilla [3] also noted that, in a homogeneous collisionless plasma, the dielectric tensor always satisfies the Onsager symmetry relations independently of the particular form of the equilibrium distribution function. Gaelzer et al. [4]

M. F. Bashir (✉)
Department of Physics, GC University Lahore,
Lahore 54000, Pakistan
e-mail: frazbashir@yahoo.com

M. F. Bashir · G. Murtaza
Salam Chair in Physics, GC University Lahore,
Lahore 54000, Pakistan

G. Murtaza
e-mail: murtaza_gcu@yahoo.com

presented a detailed derivation of the effective longitudinal dielectric constant for plasmas in inhomogeneous magnetic fields. Ziebell and Schneider [5] provided a general expression for an effective dielectric tensor satisfying the Onsager symmetry in an inhomogeneous plasma. Miyamoto [6], choosing an anisotropic streaming Maxwellian plasma, obtained the general dielectric tensor and employed it to derive the dispersion relation for different instabilities.

As is well known, the temperature is anisotropic in several environments, such as the solar wind, solar corona, auroral ionosphere, magnetosphere, astrophysical and space plasmas, and plasmas produced in recent experimental developments. These naturally occurring and laboratory plasmas generally have bi-Maxwellian or nearly bi-Maxwellian velocity distributions. Noci et al. [12] analyzed the data from the outer solar corona to show that the velocity distribution function becomes anisotropic beyond 1.8 solar radii. Pagel et al. [13] observed that the core population of solar wind is well described by a bi-Maxwellian distribution function, while the halo component is best modeled by a bi-Kappa distribution function. Schunk and Watkins [14] showed that the anisotropy in the electron-temperature distribution in the ionosphere develops above 2500 km and increases with altitude. Masood et al. [15] analysed that the electron-velocity distribution in the Earth's magnetosheath is thermally anisotropic. Cremaschini et al. [16] showed that the accretion-disk plasmas around the compact and massive objects are characterized by thermally anisotropic velocity distribution functions. In the laboratory, the incident high-energy laser wave can make the resulting plasma thermally anisotropic, because the plasma is more intensely heated in the direction of the laser-wave electric field [17–19].

The thermal anisotropy not only influences the propagation of various modes, but also induces various types of electromagnetic instabilities in a variety of plasmas including space and astrophysical plasma, fusion plasmas (both magnetic and inertial confinement) as well as in the plasma created by highly intense free electron x-ray laser pulses. In particular, the stability analysis of whistler wave and Alfvénic modes (pure Alfvé n wave, magnetosonic wave, kinetic Alfvén waves, inertial Alfvén wave, etc.) have received special attention. Whistler waves are electromagnetic waves in magnetized plasmas with frequencies below the cyclotron frequency. Whistlers are naturally produced by lightning discharges in thunderstorms. When produced near the north or south pole, they can travel from one pole to another along the Earth's magnetic lines of force through the ionosphere. As a result, lightning flashes in the Southern Hemisphere can be observed in the Northern Hemisphere [1]. Plasma-wave instruments on Voyager 2 have detected whistler-mode emissions inside and outside the magnetosphere of Saturn [20–22]. Whistlers are also observed to propagate through self-created ducts in magnetospheres [22]. Whistler modes are used to induce radio-frequency plasma discharges, and to heat plasmas in tokamaks [23] and spheromaks [24]. The Weibel instability and the Weibel instability in an ambient magnetic field (i.e., the whistler instability), which have been known for several decades [25], are of significant interest. Studies considering different particle-velocity distributions have relied on the Weibel [26–33] and whistler instabilities [34–42] to explain physical processes in different plasma environments.

Alfvén waves are believed to play major roles in certain astrophysical processes in magnetized plasmas such as ones found in the environments of stars and interstellar clouds [43]. Many phenomena in the solar atmosphere or heliosphere, planetary and cometary magnetospheres, cometary tails, Earth's ionosphere, etc., can also be regarded as manifestations of linear or nonlinear Alfvén waves. Due to their incompressibility and low reflectivity in the solar atmosphere [44], Alfvén waves have been invoked as the most promising wave mechanism to explain the heating of Sun's outer atmosphere, or corona, to millions of degrees and the acceleration of the solar wind to hundreds of kilometers per second [45]. Gekelman has studied Alfvén waves and their relationship to space observations in the laboratory [46]. One of the most important instabilities that excite Alfvén waves in a hot plasma is the so-called fire-hose instability, driven by the plasma temperature anisotropy. Since the thermal anisotropy is an intrinsic characteristic of magnetized plasmas, especially in the cases of collisionless plasmas such as astrophysical and space plasmas, the fire-hose instability has many implications in these plasmas, and has been discussed in the literature on the basis of the Vlasov kinetic theory. The fire-hose instability in magnetized thermal plasmas has been studied by a number of authors [47–50]. Kinetic Alfvén waves (KAWs) are produced due to charge separation when the perpendicular wavelength becomes comparable to the ion gyroradius and show dispersive character for oblique propagation [51]. Bashir et al. discussed the effect of thermal anisotropy on the propagation characteristics of KAWs in both the kinetic and the inerial regimes [52]. Various other aspects of the KAWs have been studied by several authors [53–70]. Recent theoretical and experimental advances focused on the wave propagation of KAWs in different regimes have associated the morphology of the wave with the generation mechanism proposed by Gekelman et al. [71].

Here, we present an extended review on plasma waves and instabilities and discuss the anisotropic response of the general relativistic dielectric tensor as well as the Onsager symmetric properties for a homogeneous magnetized collisionless plasma for an arbitrary distribution function. Considering non-relativistic bi-Maxwellian distributions, we simplify the analytical expressions for the components of dielectric tensor in the limit $|\xi_{n\alpha}| \gg 1$, where $\xi_{n\alpha} = (\omega - n\Omega_\alpha)/(k_\parallel v_{t\parallel\alpha})$; this allows easier switching to parallel or perpendicular propagation. We moreover obtain the dispersion relations for various modes and instabilities, along with their graphical representation, from the simplified components of the dielectric tensor under the appropriate conditions. For example, (i) for parallel propagation, we derive the dispersion relations for the R- and L-waves, whistler wave, Alfvén wave, Langmuir wave, Alfvén wave instability, whistler instabilities, and Weibel instabilities, along with the conditions for instability; (ii) for perpendicular propagation, the general dispersion relations for the X-mode, O-mode and Bernstein mode are derived; (iii) for oblique propagation, we derive the general dispersion relations for the Kinetic Alfvén waves (KAWs) in the kinetic and inertial regimes, and for the fast mode. In addition, we recover a number of special cases for the general fast-mode dispersion relation under appropriate conditions. We also discuss the fast mode instability for oblique propagation.

The plan of the paper is as follows. In Section 2, we present the general relativistic dielectric tensor and then employ the non-relativistic bi-Maxwellian distribution function to simplify the general dispersion relation for various modes and instabilities under appropriate conditions, along with their graphical representations. In Section 3 we briefly summarize and discuss the results.

2 Mathematical Model

We start out with the relativistic Vlasov equation

$$\frac{\partial f_\alpha}{\partial t} + \mathbf{v}\cdot\frac{\partial f_\alpha}{\partial \mathbf{x}} + q_\alpha\left(\mathbf{E} + \frac{\mathbf{v}\times\mathbf{B}}{c}\right)\cdot\frac{\partial f_\alpha}{\partial \mathbf{p}} = 0 \tag{1}$$

where the relativistic momentum $\mathbf{p}$ and velocity $\mathbf{v}$ are related by

$$\mathbf{p} = \gamma m\mathbf{v} \qquad \gamma = \left(1 - \frac{v^2}{c^2}\right)^{-\frac{1}{2}} = \sqrt{1 + \frac{p^2}{m^2c^2}}$$

$$\mathbf{v} = \frac{c\mathbf{p}}{\sqrt{m^2c^2 + p^2}} \tag{2}$$

Equation (1), combined with the Maxwell Equations

$$\nabla\times\mathbf{E} = -\frac{1}{c}\frac{\partial\mathbf{B}}{\partial t} \tag{3}$$

$$\nabla\times\mathbf{B} = \frac{1}{c}\frac{\partial\mathbf{E}}{\partial t} + \frac{4\pi}{c}\mathbf{J}, \tag{4}$$

describe the dynamics of the plasma system.

Linearizing (1), (3), and (4), taking the Fourier-Laplace transform, assuming the ambient magnetic field $\mathbf{B}_0$ along z- direction and the wavenumber vector $\mathbf{k}$ in the x-z plane, we obtain the perturbed distribution function

$$f_{1\alpha} = \frac{q_\alpha}{\Omega_\alpha}\int_{\pm\infty}^{\phi}\exp\left[\frac{1}{\Omega_\alpha}\left\{\left(s + ik_\parallel v_\parallel\right)(\phi - \phi') + ik_\perp v_\perp(\sin\phi - \sin\phi')\right\}\right] \times\left(\left(\mathbf{E}_1 + \frac{\mathbf{v}'\times\mathbf{B}_1}{c}\right)\cdot\frac{\partial f_{0\alpha}}{\partial\mathbf{p}'}\right)d\phi'$$

and the dyadic equation

$$\left(s^2 + c^2k^2\right)\mathbf{E}_1 - c^2\mathbf{k}(\mathbf{k}.\mathbf{E}_1) + 4\pi s\mathbf{J} = \mathbf{0} \tag{5}$$

Given the distribution function $f_{1\alpha}$, we can calculate the current density

$$\mathbf{J} = \overleftrightarrow{\sigma}.\mathbf{E}_1 = \sum_\alpha q_\alpha n_{0\alpha}\int\mathbf{v}\,f_{1\alpha}d^3p,$$

where $\overleftrightarrow{\sigma}$ is the conductivity tensor.

We can rewrite the dyadic equation (5) in terms of the dielectric permittivity tensor $\overleftrightarrow{\varepsilon}$ [6] as

$$\left[\varepsilon_{ij} - N^2\left(\delta_{ij} - \frac{N_iN_j}{N^2}\right)\right]E_j = 0, \tag{6}$$

where

$$\epsilon_{ij} \equiv \delta_{ij} + \frac{4\pi\sigma_{ij}}{s} = \delta_{ij} - \sum_{n=-\infty}^{\infty} M_{ij} + L_{ij}, \tag{7}$$

with

$$M_{ij} = \frac{2\pi}{s}\sum_\alpha m_\alpha\omega_{p\alpha}^2\int_{-\infty}^{\infty}dp_\parallel\int_0^{\infty}p_\perp dp_\perp \times\sum_{n=-\infty}^{\infty}\frac{\chi_1}{s + ik_\parallel v_\parallel + in\Omega_\alpha}\times \times\begin{pmatrix}\frac{n^2}{z^2}v_\perp[J_n(z)]^2 & \frac{in}{z}v_\perp J_n(z)J_n'(z) & \frac{n}{z}v_\parallel[J_n(z)]^2\\ -\frac{in}{z}v_\perp J_n(z)J_n'(z) & v_\perp[J_n'(z)]^2 & -iv_\parallel J_n(z)J_n'(z)\\ \frac{n}{z}v_\parallel[J_n(z)]^2 & iv_\parallel J_n(z)J_n'(z) & \frac{v_\parallel^2}{v_\perp}[J_n(z)]^2\end{pmatrix},$$

the only nonzero component of L_{ij} being

$$L_{zz} = \frac{2\pi}{s^2}\sum_{\alpha} m_\alpha \omega_{p\alpha}^2 \int_{-\infty}^{\infty} dp_\parallel \int_0^{\infty} p_\perp dp_\perp \times \left[\frac{v_\parallel}{v_\perp}\left(v_\parallel \frac{\partial f_{0\alpha}}{\partial p_\perp} - v_\perp \frac{\partial f_{0\alpha}}{\partial p_\parallel}\right)\right]$$

Here we have used the following properties of the Bessel functions:

$$\sum_{n=-\infty}^{\infty} n[J_n(z)]^2 = 0, \quad \sum_{n=-\infty}^{\infty} J_n(z)J_n'(z) = 0,$$

$$\sum_{n=-\infty}^{\infty} [J_n(z)]^2 = 1,$$

and defined

$$\chi_1 = \left\{\frac{\partial f_{0\alpha}}{\partial p_\perp} + \frac{i k_\parallel}{s}\left(v_\parallel \frac{\partial f_{0\alpha}}{\partial p_\perp} - v_\perp \frac{\partial f_{0\alpha}}{\partial p_\parallel}\right)\right\}.$$

$N = \frac{ck}{\omega}$ is the total refractive index, whose components are $N_{i,j} = ck_{i,\ j}/\omega$, while $\omega_{p\alpha}^2 = 4\pi n_{o\alpha} e^2/m_{0\alpha}$ is the non-relativistic plasma frequency, and Ω_α [$= \Omega_{0\alpha}/\gamma = q_\alpha B_0/(\gamma m_{0\alpha} c)$] is the relativistic cyclotron frequency.

Equation (7) gives the general relativistic dielectric tensor in a homogeneous magnetized plasma for an arbitrary equilibrium distribution function $f_{0\alpha}$. From (7), it is clear that χ_1 (only for $k_\parallel \neq 0$) and L_{zz} contain the anisotropic modification factor $(v_\parallel \frac{\partial f_{0\alpha}}{\partial p_\perp} - v_\perp \frac{\partial f_{0\alpha}}{\partial p_\parallel})$. This factor stems from the term $(\mathbf{v} \times \mathbf{B}_1) \cdot \frac{\partial f_{0\alpha}}{\partial \mathbf{p}}$ in the linearized Vlasov equation, which vanishes for isotropic velocity distributions or under electrostatic conditions, i.e., for $\mathbf{k} \| \mathbf{E}$. The same term however survives for those electromagnetic modes in which the ambient magnetic field is perpendicular to the perturbed magnetic field, i.e., for $\mathbf{B}_1 \perp \mathbf{B}_0$, for any arbitrary anisotropic distribution (from non-relativistic to relativistic regimes). From the Maxwell Equations, it is clear that generation of perturbed magnetic field depends upon the propagation direction and the polarizations of electric field. As illustrated by Fig. 1 the R- and L-waves and the waves derived from them for parallel propagation, and the O-mode for perpendicular propagation satisfy the requirement that the ambient magnetic field be perpendicular to the perturbed magnetic field. The same is evident from (7), since χ_1 exhibits the thermal anisotropy effect for $k_\parallel \neq 0$ only. In the case of the O-mode (i.e., $\epsilon_{zz} - N_\perp^2 = 0$), the anisotropy effect comes from the L_{zz} component. For parallel propagation of electrostatic modes (i.e., for $\epsilon_{zz} = 0$),

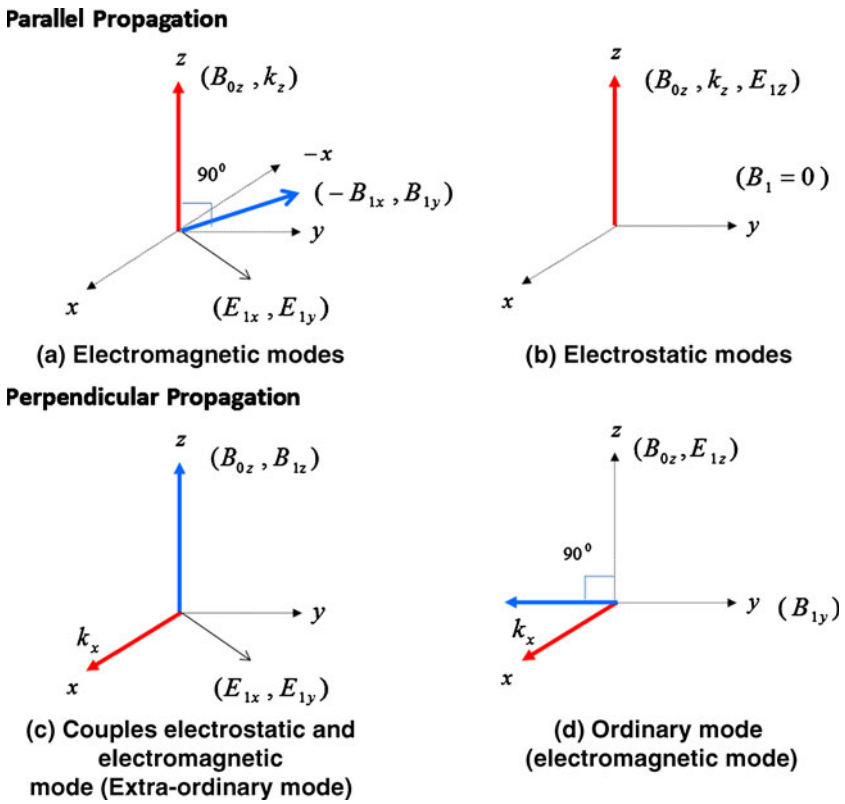

Fig. 1 (*Color online*) Geometrical representation of different modes. In all panels, the z axis is aligned with the ambient field $\vec{B}_0$. The arrows indicate the directions of the electric field $\vec{E}_1$, magnetic field $\vec{B}_1$ (*blue bold arrow*) and the wave vector $\vec{k}$ (*red bold arrow*). Panels (**a**) and (**b**) show an electromagnetic mode and an electrostatic mode propagating in the z direction and. Panel (**c**) depicts an extraordinary mode, the coupling of an electrostatic and an electromagnetic modes, propagating in the x direction. Panel (**d**) shows an ordinary mode propagating in the x direction

a contribution from the anisotropic effect is found in M_{ij} and another is found in L_{ij}, but the two contributions cancel each other. The obliquely propagating electromagnetic modes always contain the anisotropic modification.

In the following section we will prove that for a non-relativistic bi-Maxwellian distribution, only the modes whose perturbed magnetic field is perpendicular to the ambient field are modified by the thermal anisotropy.

A remarkable property of the general dielectric tensor is described by the Onsager symmetry relations,

$$\epsilon_{xy} = -\epsilon_{yx}, \quad \epsilon_{xz} = \epsilon_{zx} \text{ and } \epsilon_{yz} = -\epsilon_{zy}$$

which is always satisfied by the hot-plasma dielectric tensor, independently of the choice of equilibrium distribution function $f_{0\alpha}$.

The above discussion on the anisotropic response of dielectric tensor and Onsager symmetry relations are valid for arbitrary anisotropic distributions and cover magnetized-plasma environments ranging from the non-relativistic to the ultra-relativistic regimes.

2.1 General Dielectric Tensor for Non-relativistic Bi-Maxwellian Distribution

We shall now derive the general dielectric tensor for a non-relativistic bi-Maxwellian plasma. The non-relativistic bi-Maxwellian distribution function is

$$f_{0\alpha} = \frac{1}{2\pi m_\alpha T_{\perp\alpha} \left(2\pi m_\alpha T_{\parallel\alpha}\right)^{\frac{1}{2}}} \exp\left[-\frac{p_\perp^2}{2m_\alpha T_{\perp\alpha}} - \frac{p_\parallel^2}{2m_\alpha T_{\parallel\alpha}}\right] \tag{8}$$

Once the integrations over $p_\parallel$ and $p_\perp$ are carried out, with the help of the Onsager symmetry relations, the following general dispersion relation is obtained [52]

$$\begin{vmatrix} \epsilon_{xx} - N_\parallel^2 & \epsilon_{xy} & \epsilon_{xz} + N_\parallel N_\perp \\ -\epsilon_{xy} & \epsilon_{yy} - N^2 & \epsilon_{yz} \\ \epsilon_{xz} + N_\parallel N_\perp & -\epsilon_{yz} & \epsilon_{zz} - N_\perp^2 \end{vmatrix} = 0 \tag{9}$$

where

$$\epsilon_{xx} = 1 + \sum_\alpha \frac{\omega_{p\alpha}^2}{\omega^2} \sum_{n=-\infty}^{\infty} \frac{n^2}{\lambda_\alpha} \Gamma_n(\lambda_\alpha) \times \left\{ \xi_{0\alpha}\, Z\left(\xi_{n\alpha}\right) - \frac{Z'\left(\xi_{n\alpha}\right)}{2} \left(\frac{T_{\perp\alpha}}{T_{\parallel\alpha}} - 1\right) \right\} \tag{10}$$

$$\varepsilon_{yy} = 1 + \sum_\alpha \frac{\omega_{p\alpha}^2}{\omega^2} \sum_{n=-\infty}^{\infty} \left(\frac{n^2 \Gamma_n(\lambda_\alpha)}{\lambda_\alpha} - 2\lambda_\alpha\, \Gamma_n'(\lambda_\alpha) \right) \times \left\{ \xi_{0\alpha}\, Z\left(\xi_{n\alpha}\right) - \frac{Z'\left(\xi_{n\alpha}\right)}{2} \left(\frac{T_{\perp\alpha}}{T_{\parallel\alpha}} - 1\right) \right\} \tag{11}$$

$$\varepsilon_{zz} = 1 - \sum_\alpha \frac{\omega_{p\alpha}^2}{\omega^2} \xi_{0\alpha} \sum_{n=-\infty}^{\infty} \Gamma_n(\lambda_\alpha) \xi_{n\alpha} Z'\left(\xi_{n\alpha}\right) \times \left\{ 1 + \frac{n\Omega_{0\alpha}}{\omega} \left(\frac{T_{\parallel\alpha}}{T_{\perp\alpha}} - 1\right) \right\} \tag{12}$$

$$\varepsilon_{xy} = i \sum_\alpha \frac{\omega_{p\alpha}^2}{\omega^2} \sum_{n=-\infty}^{\infty} n \Gamma_n'(\lambda_\alpha) \times \left\{ \xi_{0\alpha}\, Z\left(\xi_{n\alpha}\right) - \frac{Z'\left(\xi_{n\alpha}\right)}{2} \left(\frac{T_{\perp\alpha}}{T_{\parallel\alpha}} - 1\right) \right\} \tag{13}$$

$$\varepsilon_{xz} = -\sum_\alpha \frac{\omega_{p\alpha}^2}{\omega^2} \frac{v_{t_{\parallel\alpha}}}{v_{t_{\perp\alpha}}} \sum_{n=-\infty}^{\infty} \frac{n\Gamma_n(\lambda_\alpha)}{\sqrt{2\lambda_\alpha}} \times \left\{ \xi_{0\alpha} + \xi_{n\alpha} \left(\frac{T_{\perp\alpha}}{T_{\parallel\alpha}} - 1\right) \right\} Z'\left(\xi_{n\alpha}\right) \tag{14}$$

$$\varepsilon_{yz} = i \sum_\alpha \frac{v_{t_{\parallel\alpha}}}{v_{t_{\perp\alpha}}} \frac{\omega_{p\alpha}^2}{\omega^2} \sum_{n=-\infty}^{\infty} \sqrt{\frac{\lambda_\alpha}{2}}\, \Gamma_n'(\lambda_\alpha) \times \left\{ \xi_{0\alpha} + \xi_{n\alpha} \left(\frac{T_{\perp\alpha}}{T_{\parallel\alpha}} - 1\right) \right\} Z'\left(\xi_{n\alpha}\right) \tag{15}$$

Here, ϵ_{ij} is the permittivity dielectric tensor. The parameters in (10)–(15) are defined as follows:

$$\xi_{n\alpha} = \frac{\omega - n\Omega_{0\alpha}}{k_\parallel v_{t\parallel\alpha}}, \quad \lambda_\alpha = \frac{k_\perp^2 v_{t\perp\alpha}^2}{2\Omega_{0\alpha}^2}, \quad v_{t\parallel\alpha} = \left(2T_{\parallel\alpha}/m_\alpha\right)^{1/2} \text{ and } \quad v_{t\perp\alpha} = \left(2T_{\perp\alpha}/m_\alpha\right)^{1/2} \tag{16}$$

The results of the integration over $p_\perp$ are expressed in terms of the functions $\Gamma_n(\lambda_\alpha)$ and $\Gamma_n'(\lambda_\alpha)$, which are related to the modified Bessel function $I_n(\lambda_\alpha)$ by the expressions $\Gamma_n(\lambda_\alpha) = e^{-\lambda_\alpha} I_n(\lambda_\alpha)$ and $\Gamma_n'(\lambda_\alpha) = e^{-\lambda_\alpha}(I_n'(\lambda_\alpha) - I_n(\lambda_\alpha))$. The integration over $p_\parallel$ introduces the plasma dispersion functions $Z(\xi_{n\alpha})$ and $Z'(\xi_{n\alpha})$ [72]. For the isotropic case, the dielectric permittivity tensor ϵ_{ij} reduces to the usual textbook form [1, 3].

2.2 Dispersion Relations for various Modes and Instabilities

In the limit $|\xi_{n\alpha}| \gg 1$, the general dispersion relation is further simplified, and the dispersion relations for

various modes and instabilities can be derived. In that limit, the plasma dispersion function assumes the form

$$Z(\xi_{n\alpha}) = -\frac{1}{\xi_{n\alpha}} - \frac{1}{2\xi_{n\alpha}^3} - \frac{3}{4\xi_{n\alpha}^5} + \cdots = -\sum_{l=0}^{\infty} \frac{(2l+1)!!}{(2l+1)\ 2^l} \left(\frac{k_\parallel v_{t_{\parallel\alpha}}}{\omega - n\Omega_{0\alpha}}\right)^{2l+1} \text{for } |\xi_{n\alpha}| \gg 1$$

For $|\xi_{n\alpha}| \gg 1$, the components of the tensor in (9) take the form

$$\epsilon_{xx} = 1 - \sum_\alpha \frac{\omega_{p\alpha}^2}{\omega^2} \sum_{n=1}^{\infty} \frac{n^2}{\lambda_\alpha} \Gamma_n(\lambda_\alpha) \sum_{l=0}^{\infty} \frac{(2l+1)!!}{(2l+1)} \times \left\{ \frac{\omega \left(k_\parallel v_{t_{\parallel\alpha}}\right)^{2l}}{(\omega - n\Omega_{0\alpha})^{2l+1}} + \frac{\omega \left(k_\parallel v_{t_{\parallel\alpha}}\right)^{2l}}{(\omega + n\Omega_{0\alpha})^{2l+1}} + \frac{(2l+1)}{2^{l+1}} \times \left(\frac{T_{\perp\alpha}}{T_{\parallel\alpha}} - 1\right) \left(\left(\frac{k_\parallel v_{t_{\parallel\alpha}}}{\omega - n\Omega_{0\alpha}}\right)^{2l+2} + \left(\frac{k_\parallel v_{t_{\parallel\alpha}}}{\omega + n\Omega_{0\alpha}}\right)^{2l+2} \right) \right\} \tag{17}$$

$$\varepsilon_{yy} = 1 - \left[\sum_\alpha \frac{\omega_{p\alpha}^2}{\omega^2} \sum_{n=1}^{\infty} \left(\frac{n^2 \Gamma_n(\lambda_\alpha)}{\lambda_\alpha} - 2\lambda_\alpha\, \Gamma_n'(\lambda_\alpha) \right) \times \sum_{l=0}^{\infty} \frac{(2l+1)!!}{(2l+1)} \left\{ \frac{\omega \left(k_\parallel v_{t_{\parallel\alpha}}\right)^{2l}}{(\omega - n\Omega_{0\alpha})^{2l+1}} + \frac{\omega \left(k_\parallel v_{t_{\parallel\alpha}}\right)^{2l}}{(\omega + n\Omega_{0\alpha})^{2l+1}} + \frac{(2l+1)}{2^{l+1}} \left(\frac{T_{\perp\alpha}}{T_{\parallel\alpha}} - 1\right) \times \left(\left(\frac{k_\parallel v_{t_{\parallel\alpha}}}{\omega - n\Omega_{0\alpha}}\right)^{2l+2} + \left(\frac{k_\parallel v_{t_{\parallel\alpha}}}{\omega + n\Omega_{0\alpha}}\right)^{2l+2} \right) \right\} \right] - 2 \sum_\alpha \frac{\omega_{p\alpha}^2}{\omega^2} \lambda_\alpha\, \Gamma_0'(\lambda_\alpha) \times \left\{ \xi_{0\alpha}\, Z(\xi_{0\alpha}) - \frac{Z'(\xi_{0\alpha})}{2} \left(\frac{T_{\perp\alpha}}{T_{\parallel\alpha}} - 1\right) \right\} \tag{18}$$

$$\varepsilon_{zz} = 1 - \sum_\alpha \frac{\omega_{p\alpha}^2}{\omega^2} \Gamma_0(\lambda_\alpha) \xi_{0\alpha}^2\, Z'(\xi_{0\alpha}) - \sum_\alpha \frac{\omega_{p\alpha}^2}{\omega} \sum_{n=1}^{\infty} \Gamma_n(\lambda_\alpha) \sum_{l=0}^{\infty} \frac{(2l+1)!!}{2^l} \times \left[\frac{\left(k_\parallel v_{t_{\parallel\alpha}}\right)^{2l}}{(\omega - n\Omega_{0\alpha})^{2l+1}} + \frac{\left(k_\parallel v_{t_{\parallel\alpha}}\right)^{2l}}{(\omega + n\Omega_{0\alpha})^{2l+1}} + \frac{n\Omega_{0\alpha}}{\omega} \left(\frac{T_{\parallel\alpha}}{T_{\perp\alpha}} - 1\right) \times \left(\frac{\left(k_\parallel v_{t_{\parallel\alpha}}\right)^{2l}}{(\omega - n\Omega_{0\alpha})^{2l+1}} - \frac{\left(k_\parallel v_{t_{\parallel\alpha}}\right)^{2l}}{(\omega + n\Omega_{0\alpha})^{2l+1}} \right) \right] \tag{19}$$

$$\varepsilon_{xy} = -\varepsilon_{yx} = -i \sum_\alpha \frac{\omega_{p\alpha}^2}{\omega^2} \sum_{n=1}^{\infty} n\Gamma_n'(\lambda_\alpha) \sum_{l=0}^{\infty} \frac{(2l+1)!!}{(2l+1)} \times \left\{ \frac{\omega \left(k_\parallel v_{t_{\parallel\alpha}}\right)^{2l}}{(\omega - n\Omega_{0\alpha})^{2l+1}} - \frac{\omega \left(k_\parallel v_{t_{\parallel\alpha}}\right)^{2l}}{(\omega + n\Omega_{0\alpha})^{2l+1}} + \frac{(2l+1)}{2^{l+1}} \left(\frac{T_{\perp\alpha}}{T_{\parallel\alpha}} - 1\right) \left(\left(\frac{k_\parallel v_{t_{\parallel\alpha}}}{\omega - n\Omega_{0\alpha}}\right)^{2l+2} - \left(\frac{k_\parallel v_{t_{\parallel\alpha}}}{\omega + n\Omega_{0\alpha}}\right)^{2l+2} \right) \right\} \tag{20}$$

$$\varepsilon_{xz} = \varepsilon_{zx} = -\sum_\alpha \frac{\omega_{p\alpha}^2}{\omega} \frac{v_{t_{\parallel\alpha}}}{v_{t_{\perp\alpha}}} \sum_{n=1}^{\infty} \frac{n\Gamma_n(\lambda_\alpha)}{\sqrt{2\lambda_\alpha}} \sum_{l=0}^{\infty} \frac{(2l+1)!!}{2^l} \times \left[\frac{T_{\perp\alpha}}{T_{\parallel\alpha}} \left\{ \frac{\left(k_\parallel v_{t_{\parallel\alpha}}\right)^{2l+1}}{(\omega - n\Omega_{0\alpha})^{2l+2}} - \frac{\left(k_\parallel v_{t_{\parallel\alpha}}\right)^{2l+1}}{(\omega + n\Omega_{0\alpha})^{2l+2}} \right\} - \frac{n\Omega_{0\alpha}}{\omega} \left(\frac{T_{\perp\alpha}}{T_{\parallel\alpha}} - 1\right) \times \left\{ \frac{\left(k_\parallel v_{t_{\parallel\alpha}}\right)^{2l+1}}{(\omega - n\Omega_{0\alpha})^{2l+2}} + \frac{\left(k_\parallel v_{t_{\parallel\alpha}}\right)^{2l+1}}{(\omega + n\Omega_{0\alpha})^{2l+2}} \right\} \right] \tag{21}$$

$$\varepsilon_{yz} = -\varepsilon_{zy} = i \sum_\alpha \frac{v_{t_\parallel}}{v_{t\perp}} \frac{\omega_{p\alpha}^2}{\omega} \sum_{n=1}^{\infty} \sqrt{\frac{\lambda_\alpha}{2}}\, \Gamma_n'(\lambda_\alpha) \sum_{l=0}^{\infty} \frac{(2l+1)!!}{2^l} \times \left[\frac{T_{\perp\alpha}}{T_{\parallel\alpha}} \left\{ \frac{\left(k_\parallel v_{t_{\parallel\alpha}}\right)^{2l+1}}{(\omega - n\Omega_{0\alpha})^{2l+2}} + \frac{\left(k_\parallel v_{t_{\parallel\alpha}}\right)^{2l+1}}{(\omega + n\Omega_{0\alpha})^{2l+2}} \right\} - \frac{n\Omega_{0\alpha}}{\omega} \left(\frac{T_{\perp\alpha}}{T_{\parallel\alpha}} - 1\right) \times \left\{ \frac{\left(k_\parallel v_{t_{\parallel\alpha}}\right)^{2l+1}}{(\omega - n\Omega_{0\alpha})^{2l+2}} - \frac{\left(k_\parallel v_{t_{\parallel\alpha}}\right)^{2l+1}}{(\omega + n\Omega_{0\alpha})^{2l+2}} \right\} \right] \tag{22}$$

In (17)–(22), we have separated the $n = 0$ terms from those with $n > 0$ and $n < 0$. For $n = 0$, we have retained the plasma dispersion function to be used later. We have also used the symmetry properties of the modified Bessel function, i .e., $\Gamma_n(\lambda_\alpha) = \Gamma_{-n}(\lambda_\alpha)$ and $\Gamma_n'(\lambda_\alpha) = \Gamma_{-n}'(\lambda_\alpha)$. Each component of the ϵ_{ij} tensor contributes to oblique propagation, since both components of the wave-number vector, $k_\perp$ and $k_\parallel$ are present via the $\Gamma_n(\lambda_\alpha)$ and $Z(\xi_{n\alpha})$ functions, respectively, and contain the effects of thermal anisotropy.

Sections 2.2.1, 2.2.2 and 2.2.3 discuss the parallel, perpendicular and oblique propagations, respectively, for the limiting case $|\xi_{n\alpha}| \gg 1$.

2.2.1 Parallel Propagation

Taking $k_\perp = 0$ in (17)–(22), we obtain the equations

$$\epsilon_{xx} = \varepsilon_{yy} = 1 - \sum_\alpha \frac{\omega_{p\alpha}^2}{2\omega^2} \sum_{l=0}^{\infty} \frac{(2l+1)!!}{(2l+1)} \times \left\{ \frac{\omega \left(k_\parallel v_{t_{\parallel\alpha}}\right)^{2l}}{(\omega - \Omega_{0\alpha})^{2l+1}} + \frac{\omega \left(k_\parallel v_{t_{\parallel\alpha}}\right)^{2l}}{(\omega + \Omega_{0\alpha})^{2l+1}} + \frac{(2l+1)}{2^{l+1}} \left(\frac{T_{\perp\alpha}}{T_{\parallel\alpha}} - 1\right) \left(\left(\frac{k_\parallel v_{t_{\parallel\alpha}}}{\omega - \Omega_{0\alpha}}\right)^{2l+2} + \left(\frac{k_\parallel v_{t_{\parallel\alpha}}}{\omega + \Omega_{0\alpha}}\right)^{2l+2} \right) \right\} \quad (23)$$

$$\varepsilon_{xy} = -\varepsilon_{yx} = -i \sum_\alpha \frac{\omega_{p\alpha}^2}{2\omega^2} \sum_{l=0}^{\infty} \frac{(2l+1)!!}{(2l+1)} \times \left\{ \frac{\omega \left(k_\parallel v_{t_{\parallel\alpha}}\right)^{2l}}{(\omega - \Omega_{0\alpha})^{2l+1}} - \frac{\omega \left(k_\parallel v_{t_{\parallel\alpha}}\right)^{2l}}{(\omega + \Omega_{0\alpha})^{2l+1}} + \frac{(2l+1)}{2^{l+1}} \left(\frac{T_{\perp\alpha}}{T_{\parallel\alpha}} - 1\right) \left(\left(\frac{k_\parallel v_{t_{\parallel\alpha}}}{\omega - \Omega_{0\alpha}}\right)^{2l+2} - \left(\frac{k_\parallel v_{t_{\parallel\alpha}}}{\omega + \Omega_{0\alpha}}\right)^{2l+2} \right) \right\} \quad (24)$$

$$\varepsilon_{zz} = 1 - \sum_\alpha \frac{\omega_{p\alpha}^2}{\omega^2} \xi_{0\alpha}^2 \, Z'(\xi_{o\alpha}) \quad (25)$$

and $\varepsilon_{xz} = \varepsilon_{yz} = 0$

Here we have expanded the modified Bessel function as follows:

$$\Gamma_n(\lambda_\alpha) = \frac{1}{n!}\left(\frac{\lambda_\alpha}{2}\right)^n, \quad \Gamma_n'(\lambda_\alpha) = \frac{n}{n!2}\left(\frac{\lambda_\alpha}{2}\right)^{n-1}\left(1 - \frac{\lambda_\alpha}{n}\right)$$

and $\Gamma_0'(\lambda_\alpha) = -1$

and noted that only the $n = 1$ terms survive for $k_\perp = 0$.

Therefore, for parallel propagation, the general dispersion relation in (9) reduces to the form

$$\left[\left(\epsilon_{xx} - N_\parallel^2\right)^2 + \epsilon_{xy}^2\right]\epsilon_{zz} = 0, \quad (26)$$

which decouples the electrostatic modes

$$\epsilon_{zz} = 0, \quad (27)$$

from the electromagnetic modes

$$N_\parallel^2 = \epsilon_{xx} \pm i\epsilon_{xy}. \quad (28)$$

The upper (+) and the lower (−) signs correspond to the R- and L- waves, respectively. While the dispersion relation for R- and L- waves retain the thermal anisotropy effect, the electrostatic mode exhibits no such effect, as expected.

R- and L- Waves Using (23) and (24), we may rewrite the dispersion relation for the R- and L- waves in (28) in the form

$$\frac{c^2 k_\parallel^2}{\omega^2} = 1 - \sum_\alpha \frac{\omega_{p\alpha}^2}{\omega^2} \sum_{l=0}^{\infty} \frac{(2l+1)!!}{(2l+1)} \left(\frac{k_\parallel v_{t_{\parallel\alpha}}}{\omega \pm \Omega_{0\alpha}}\right)^{2l} \times \left\{ \frac{\omega}{\omega \pm \Omega_{0\alpha}} + \frac{(2l+1)}{2^{l+1}} \left(\frac{T_{\perp\alpha}}{T_{\parallel\alpha}} - 1\right) \left(\frac{k_\parallel^2 v_{t_{\parallel\alpha}}^2}{(\omega \pm \Omega_{0\alpha})^2}\right) \right\} \quad (29)$$

This equation represents the general dispersion relation for R- and L- waves incorporating the thermal anisotropy as well as the higher-order thermal effects parallel to the ambient magnetic field. To retrieve the cold plasma result, we may assume the plasma to be isotropic and take only the leading term, i.e., $l = 0$. Further, with $\Omega_{0\alpha} = 0$, the structure of both the R- and the L- waves vanishes altogether and we obtain the dispersion relation for an unmagnetized plasma. Since the dielectric tensor for more than one species is additive, we can also solve the dispersion relation for a multi-species plasma.

The graphical representations of electron R- and L- waves with $l = 0$ in (30) are shown in Figs. 2 and 3, respectively. The dotted curve represents the standard isotropic R- and L- waves and the other curves depict the deviation from the isotropic case. We observe that

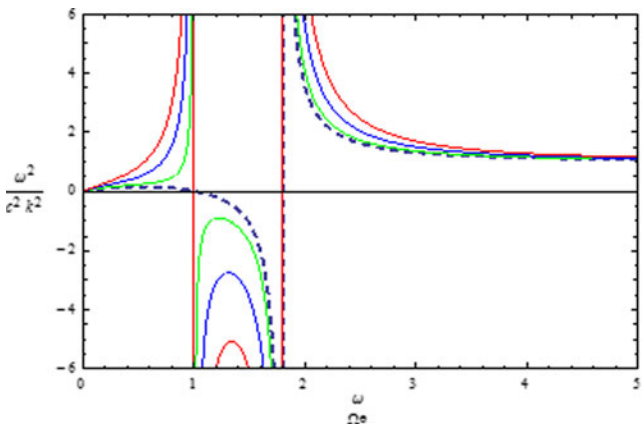

Fig. 2 (*Color online*) Graphical illustration of circularly polarized electron R-wave. The normalized phase velocity ω^2/c^2k^2 as function of normalized wave frequency ω/Ω_{0e} which depicts the deviation from isotropic case with the change of thermal anisotropy values (i.e., A=0 (*dotted*), 5 (*green*), 20 (*blue*), 40 (*red*)) choosing the parameters $\omega_{pe}/\Omega_{0e} = 1.2$, $v_{t\parallel}/c = 0.2$ & $A = \left(T_{\perp e}/T_{\parallel e}\right) - 1$. The plot shows that the phase velocity of R-wave increases with the increase in temperature anisotropy

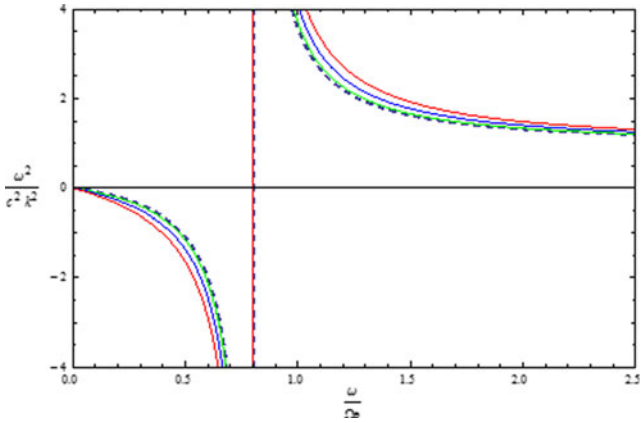

Fig. 3 (*Color online*) Graphical illustration of circularly polarized electron L-wave. The normalized phase velocity ω^2/c^2k^2 as function of normalized wave frequency ω/Ω_{0e} which depicts the deviation from isotropic case with the change of thermal anisotropy values (i.e., A=0 (*dotted*), 5 (*green*), 20 (*blue*), 40 (*red*)) choosing the parameters $\omega_{pe}/\Omega_{0e} = 1.2$, $v_{t\|}/c = 0.2$ & $A = (T_{\perp e}/T_{\|e}) - 1$. The plot shows that the phase velocity of L-wave increases with the increase in temperature anisotropy

the phase velocity of the R- and L- waves increases as the magnitude of the anisotropy is increased, but the cutoff point remains unaffected. For the R-wave, the resonance disappears as anisotropy is switched on.

Whistler Mode If we keep only the leading term (i.e., $l = 0$) in (29) and assume that $\omega^2 \ll c^2k_\|^2$, the dispersion relation for an electron R-wave reduces to

$$\omega = \frac{\Omega_{0e}\, c^2 k_\|^2}{\left(\omega_{pe}^2 + c^2 k_\|^2\right)} \left\{1 + \frac{\beta_\|}{2}\left(\frac{T_{\perp e}}{T_{\|e}} - 1\right) \frac{1}{\left(1 - \frac{\omega}{\Omega_{0e}}\right)}\right\}, \tag{30}$$

where

$$\beta_\| = \frac{c_{s_\|}^2}{V_A^2} = \frac{8\pi n_o T_{\|e}}{B_o^2}, \text{ with } \quad c_{s_\|}^2 = \frac{T_{\|e}}{m_i} \ , \quad V_A^2 = \frac{B_0^2}{4\pi n_0 m_i}. \tag{31}$$

In the low-frequency range $\Omega_{0i} < \omega < \Omega_{0e}$, (30) describes the general whistler mode

$$\omega = \frac{\dfrac{\Omega_{0e} c^2 k_\|^2}{\omega_{pe}^2}\left\{1 + \left(\dfrac{T_{\perp e}}{T_{\|e}} - 1\right)\dfrac{\beta_\|}{2}\right\}}{\left\{\left(\dfrac{c^2 k_\|^2}{\omega_{pe}^2} + 1\right) - \left(\dfrac{T_{\perp e}}{T_{\|e}} - 1\right)\dfrac{k_\|^2 v_{t_{\|e}}^2}{2\Omega_{0e}^2}\right\}}. \tag{32}$$

Here we have retained the first-order term in $\dfrac{\omega}{\Omega_{0e}}$.

For longer wavelengths, i.e., $\omega_{pe}^2 \gg c^2k_\|^2$, this dispersion relation reduces to the form

$$\omega = \frac{\dfrac{\Omega_{0e} c^2 k_\|^2}{\omega_{pe}^2}\left\{1 + \left(\dfrac{T_{\perp e}}{T_{\|e}} - 1\right)\dfrac{\beta_\|}{2}\right\}}{\left\{1 - \left(\dfrac{T_{\perp e}}{T_{\|e}} - 1\right)\dfrac{k_\|^2 v_{t_{\|e}}^2}{2\Omega_{0e}^2}\right\}}. \tag{33}$$

This is the dispersion relation for a whistler mode including the electronic thermal anisotropy effect. If we neglect the second order term in the denominator on the right-hand side, which is due to the first order term in $\dfrac{\omega}{\Omega_{0e}}$, we recover the results of Lazar et al. [42]. Figure 4 shows how the phase speed of the whistler wave is enhanced as the thermal anisotropy increases.

Non-Resonant Whistler Instability ($|\xi_{n\alpha}| \gg 1$) By considering only the leading term (i.e., $l = 0$) in the R-wave and assuming that $\omega^2 \ll c^2k_\|^2$ in (29), we obtain the following expressions for the real and imaginary parts of ω:

$$\Re\omega = \Omega_{0e}\left(1 - \frac{\omega_{pe}^2}{2\left(c^2k_\|^2 + \omega_{pe}^2\right)}\right) \tag{34}$$

and

$$\Im\omega = \omega_{pe}\frac{\sqrt{2\left(\frac{T_{\perp e}}{T_{\|e}} - 1\right)k_\|^2 v_{t_{\|e}}^2\left(c^2k_\|^2 + \omega_{pe}^2\right) - \Omega_{0e}^2\omega_{pe}^2}}{2\left(c^2k_\|^2 + \omega_{pe}^2\right)} \tag{35}$$

in agreement with Lee et al. [37] and Lazar et al. [42].

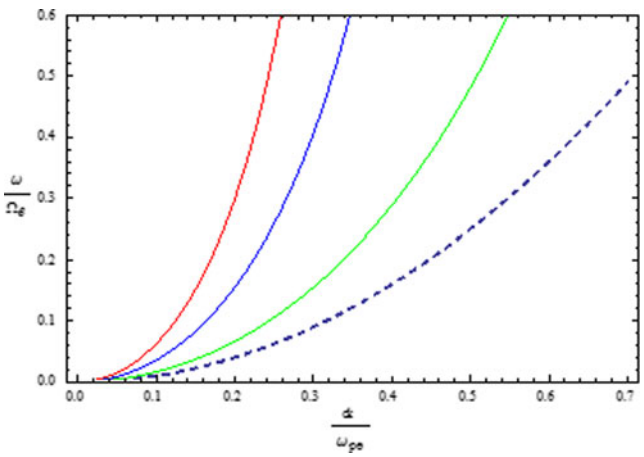

Fig. 4 (*Color online*) Normalized wave frequency ω/Ω_e of the whistler mode as a function of normalized wavenumber ck/ω_{pe} with the parameter $\omega_{pe}/\Omega_{0e} = 10$, $v_{t\|}/c = 0.05$ & $A = (T_{\perp e}/T_{\|e}) - 1$ by choosing different values of thermal anisotropy (i.e., A=0 (*dotted*), 5 (*green*), 20 (*blue*), 40 (*red*)). The wave frequency increases with the increase in temperature anisotropy

The instability occurs for wave numbers satisfying the condition

$$k_{\parallel}^2 > k_m^2 = \frac{\omega_{pe}^2}{2\,c^2}\left[\left\{1+\frac{2}{\left(\frac{T_{\perp e}}{T_{\parallel e}}-1\right)}\left(\frac{\Omega_{0e}^2}{\omega_{pe}^2}\right)\left(\frac{c^2}{v_{t_{\parallel e}}^2}\right)\right\}^{\frac{1}{2}}-1\right]. \tag{36}$$

From Fig. 5, we see that the growth rate increases as the thermal anisotropy increases, while the instability threshold is lowered. For any specific anisotropy value, the growth rate initially rises for small $k_{\parallel}$ and then saturates at large $k_{\parallel}$.

From (35), we see that the ambient magnetic field suppresses the growth rate. In the limit of large thermal anisotropy, i.e., for $\frac{T_{\perp}}{T_{\parallel}} \gg 1$, the dispersion relation reduces to

$$\Im\omega = \omega_{pe}\frac{\sqrt{2k_{\parallel}^2 v_{t_{\perp e}}^2\left(c^2k_{\parallel}^2+\omega_{pe}^2\right)-\Omega_{0e}^2\omega_{pe}^2}}{2\left(c^2k_{\parallel}^2+\omega_{pe}^2\right)}. \tag{37}$$

If the magnetic field is neglected, (37) reduces to the simpler expression

$$\Im\omega = \frac{k_{\parallel}v_{t_{\perp e}}}{\sqrt{2}}\frac{\omega_{pe}}{\sqrt{\left(c^2k_{\parallel}^2+\omega_{pe}^2\right)}}$$

which is the well-known result due to Weibel [25].

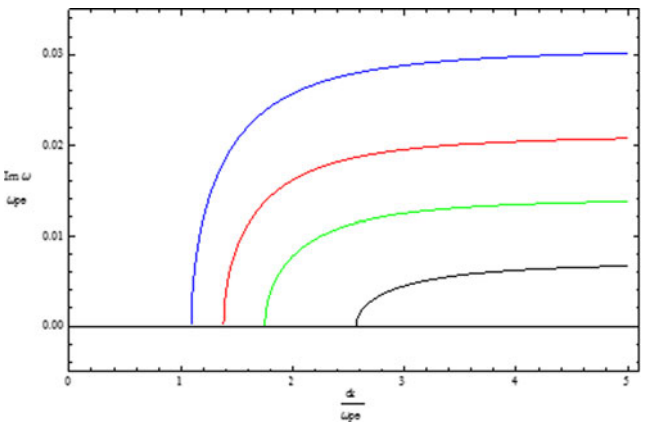

Fig. 5 (*Color online*) Normalized growth rate Im ω/ω_{pe} of non-resonant whistler instability ($|\xi_{n\alpha}| \gg 1$) as a function of normalized wavenumber ck/ω_{pe} with the parameter $\omega_{pe}/\Omega_{0e} = 1.0$, $v_{t\parallel}/c = 0.1$ & $A = \left(T_{\perp e}/T_{\parallel e}\right) - 1$ by choosing different values of thermal anisotropy (i.e., A=0 (*black*), 5 (*green*), 10 (*red*), 20 (*blue*)). By increasing the temperature anisotropy, the growth rate increases and threshold wave number shifts towards the longer wavelength and thus enlarges the wave vector domain. This instability exists only in plasma environments with $T_{\perp\alpha} > T_{\parallel\alpha}$

Alfvén Wave We now consider the dispersion relation (29) for a two-component plasma consisting of electrons and singly charged ions. In the low-frequency regime $\omega < \Omega_i$, we keep only the leading term, i.e., $l = 0$, to rewrite (29) in the form

$$\frac{\omega^2}{k_{\parallel}^2V_A^2} = \left(\frac{c^2}{V_A^2+c^2}\right)\left[1+\frac{\beta_{\parallel}}{2}\left\{\left(\frac{T_{\perp e}}{T_{\parallel}}-1\right)\left(1\pm\frac{2\omega}{\Omega_{0e}}\right)+\left(\frac{T_{\perp i}}{T_{\parallel}}-1\right)\left(1\mp\frac{2\omega}{\Omega_{0i}}\right)\right\}\right] \tag{38}$$

Here we have assumed that the two species are at the same parallel temperature and taken advantage of the small mass ratio, $m_e/m_i \ll 1$.

In the isotropic case, (38) reduces to the standard pure Alfvén mode. For frequencies satisfying $\omega \ll \Omega_{0i}$, the quadratic structure in ω vanishes, and both the R- and the L- waves follow the same dispersion relation,

$$\omega = k_{\parallel}V_A\left[1+\frac{\beta_{\parallel}}{2}\left\{\left(\frac{T_{\perp e}}{T_{\parallel}}-1\right)+\left(\frac{T_{\perp i}}{T_{\parallel}}-1\right)\right\}\right]^{\frac{1}{2}}, \tag{39}$$

a result derived by Schlickeiser and Skoda [49].

In (38) and (39), the Alfvén wave frequency is modified by acoustic effects due to the thermal anisotropy of the electrons and ions. The Alfvén phase velocity can be enhanced or reduced, depending on the intensity and signatures of the anisotropy.

From (39), it is evident that the constraint

$$\frac{2}{\beta_{\parallel}} \ll \left(1-\frac{T_{\perp e}}{T_{\parallel}}\right)+\left(1-\frac{T_{\perp i}}{T_{\parallel}}\right)$$

makes the Alfvén mode unstable, for then

$$\omega = i\,k_{\parallel}V_A\left[\frac{\beta_{\parallel}}{2}\left\{\left(1-\frac{T_{\perp e}}{T_{\parallel}}\right)+\left(1-\frac{T_{\perp i}}{T_{\parallel}}\right)\right\}-1\right]^{\frac{1}{2}}, \tag{40}$$

which describes the so-called fire-hose instability. The Alfvén-wave frequency is real for $T_{\perp e,i} > T_{\parallel e,i}$, under which condition fire-hose instabilities cannot arise.

Electrostatic Waves From (27), i.e., $\epsilon_{zz} = 0$, we obtain the dispersion relation for Langmuir waves

$$\omega^2 = \omega_{pe}^2 + \frac{3}{2}k_{\parallel}^2v_{t_{\parallel e}}^2, \tag{41}$$

where we have used the condition $|\xi_{0e}| \gg 1$ for expanding the plasma dispersion function $Z(\xi_{oe})$.

For $v_{t\|i} \ll \omega/k_\| \ll v_{t\|e}$ and $k_\|^2\lambda_{De}^2 \ll 1$, the equation $\epsilon_{zz} = 0$ yields the ion-acoustic mode

$$\omega^2 = k_\|^2 c_{s_\|}^2 \tag{42}$$

where we have used that

$$Z'(\xi_{oe}) = -2 \quad \text{for} \quad |\xi_{oe}| \ll 1, \quad Z'(\xi_{oi}) = \frac{1}{\xi_{oi}^2}$$

$$\text{for} \quad |\xi_{oi}| \gg 1 \quad \text{and} \quad c_{s_\|}^2 = \frac{T_{\|e}}{m_i}$$

The electrostatic modes, which are only affected by the temperature in the direction of propagation, are hence insensitive to the thermal anisotropy.

2.2.2 Perpendicular Propagation

Letting $k_\| = 0$ and noting that only the leading terms in the l-summation (i.e., $l = 0$) survive in (17)–(22), we obtain the expressions

$$\varepsilon_{xx} = 1 - \sum_\alpha \frac{\omega_{p\alpha}^2}{\omega^2} \sum_{n=1}^{\infty} \frac{n^2}{\lambda_\alpha} \Gamma_n(\lambda_\alpha) \left(\frac{2\omega^2}{\omega^2 - n^2\Omega_{0\alpha}^2} \right) \tag{43}$$

$$\varepsilon_{yy} = 1 - \sum_\alpha \frac{\omega_{p\alpha}^2}{\omega^2} \sum_{n=1}^{\infty} \left(\frac{n^2\Gamma_n(\lambda_\alpha)}{\lambda_\alpha} - 2\lambda_\alpha \Gamma_n'(\lambda_\alpha) \right) \times \left(\frac{2\omega^2}{\omega^2 - n^2\Omega_{0\alpha}^2} \right) + 2\sum_\alpha \frac{\omega_{p\alpha}^2}{\omega^2} \lambda_\alpha \Gamma_0'(\lambda_\alpha) \tag{44}$$

$$\varepsilon_{zz} = 1 - \sum_\alpha \frac{\omega_{p\alpha}^2}{\omega^2} \Gamma_0(\lambda_\alpha) - 2\sum_\alpha \frac{\omega_{p\alpha}^2}{\omega^2} \sum_{n=1}^{\infty} \Gamma_n(\lambda_\alpha) \times \left\{ 1 + \frac{T_{\|\alpha}}{T_{\perp\alpha}} \frac{n^2\Omega_{0\alpha}^2}{\omega^2 - n^2\Omega_{0\alpha}^2} \right\} \tag{45}$$

$$\varepsilon_{xy} = -\varepsilon_{yx} = -i\sum_\alpha \frac{\omega_{p\alpha}^2}{\omega^2} \sum_{n=1}^{\infty} n\Gamma_n'(\lambda_\alpha) \times \left(\frac{2n\omega\Omega_{0\alpha}}{\omega^2 - n^2\Omega_{0\alpha}^2} \right) \tag{46}$$

$$\varepsilon_{xz} = \varepsilon_{yz} = 0$$

In the expressions for ϵ_{yy} and ϵ_{zz}, (18) and (19), respectively, we have expanded the plasma-dispersion functions $Z(\xi_{0\alpha})$ and $Z'(\xi_{0\alpha})$ for $|\xi_{0\alpha}| \gg 1$.

Thus the general dispersion relation in (9) reduces to

$$\left[\epsilon_{xx} \left(\epsilon_{yy} - N_\perp^2 \right) + \epsilon_{xy}^2 \right] \left(\epsilon_{zz} - N_\perp^2 \right) = 0 \tag{47}$$

The above equation shows two decoupled modes: the Extraordinary (X-) mode

$$N_\perp^2 = \epsilon_{yy} \left(1 + \frac{\epsilon_{xy}^2}{\epsilon_{xx}\epsilon_{yy}} \right) \tag{48}$$

and the Ordinary (O-) mode

$$N_\perp^2 = \epsilon_{zz} \tag{49}$$

If we assume the non-diagonal components ϵ_{xy} to be much smaller than the diagonal components ϵ_{xx} and ϵ_{yy}, the X-mode dispersion relation (48) yields two decoupled modes: the purely transversal X-mode

$$N_\perp^2 = \epsilon_{yy}, \tag{50}$$

and the Bernstein mode

$$\epsilon_{xx} = 0. \tag{51}$$

Here, as in parallel propagation, we observe that the thermal anisotropy affects the dispersion relation of the O-mode (49), but does not affect the X-mode (48) or the Bernstein mode (51).

We will next discuss these three modes in more detail.

X-Mode With the help of (43), (44) and (46) we rewrite the X-mode dispersion relation (48) in the form

$$\frac{c^2k_\perp^2}{\omega^2} = \left[1 - \sum_\alpha \frac{\omega_{p\alpha}^2}{\omega^2} \sum_{n=1}^{\infty} \left(\frac{n^2\Gamma_n(\lambda_\alpha)}{\lambda_\alpha} - 2\lambda_\alpha \Gamma_n'(\lambda_\alpha) \right) \times \left(\frac{2\omega^2}{\omega^2 - n^2\Omega_{0\alpha}^2} \right) \right] - \left(\frac{\left[\sum_\alpha \frac{\omega_{p\alpha}^2}{\omega^2} \sum_{n=1}^{\infty} n\Gamma_n'(\lambda_\alpha) \left(\frac{2n\omega\Omega_{0\alpha}}{\omega^2 - n^2\Omega_{0\alpha}^2} \right) \right]^2}{\left[1 - \sum_\alpha \frac{\omega_{p\alpha}^2}{\omega^2} \sum_{n=1}^{\infty} \frac{n^2}{\lambda_\alpha} \Gamma_n(\lambda_\alpha) \left(\frac{2\omega^2}{\omega^2 - n^2\Omega_{0\alpha}^2} \right) \right]} \right), \tag{52}$$

which is the general form of the X-mode.

Figure 6 depicts the behavior of X-mode for an electron plasma. Panels (a), (c), and (e) show the behaviors for $n = 1$, and the harmonics $n = 2$, and 3, respectively,

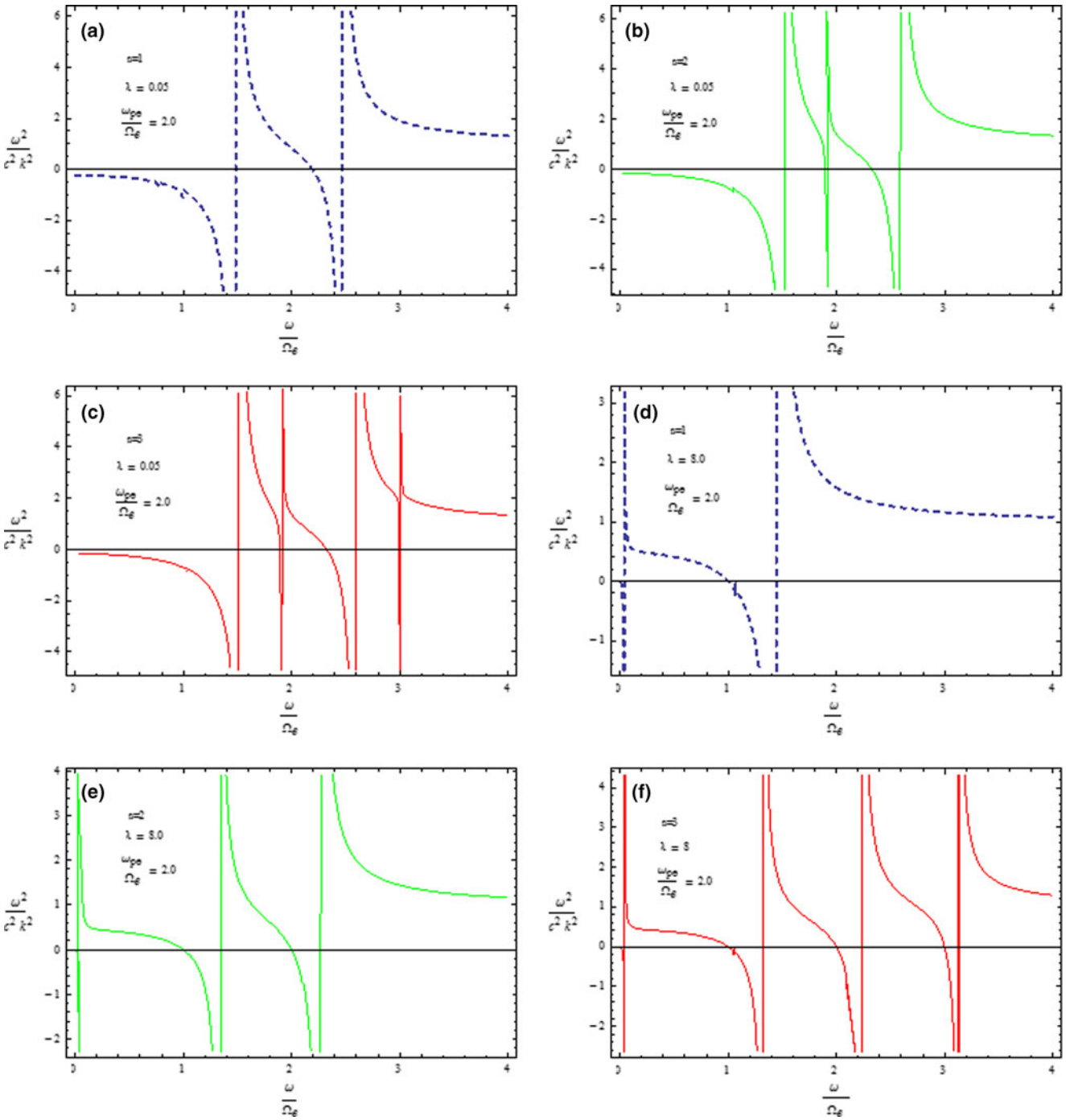

Fig. 6 (*Color online*) Behavior of X-mode for an electron plasma. Panels (**a**), (**c**), and (**e**) show the behaviors for $n = 1$ (*dotted*), and the harmonics $n = 2$ (*green*), and $n = 3$ (*red*) , respectively, with $\lambda_e = 0.05$, while panels (**b**), (**d**), and (**f**) correspond to $n = 1$, 2, and 3, respectively, with $\lambda_e = 8.0$. The number of cutoffs and resonances increases with n. The distinction between the resonance and the cutoff points is more prominent in the right panels, i.e., for the large argument. The cutoff and resonance points shift towards lower frequencies and hence expand the propagation domain as λ_e grows from 0.05 to 8.0

with $\lambda_e = 0.05$, while panels (b), (d), and (f) correspond to $n = 1$, 2, and 3, respectively, with $\lambda_e = 8.0$. The number of cutoffs and resonances increases with n. The distinction between the resonance and the cutoff points is more prominent in the right panels, i.e., for the large argument. The cutoff and resonance points shift towards lower frequencies and hence expands the propagation domain as λ_e grows from 0.05 to 8.0.

The pure transverse X-mode (i.e.,$c^2k_\perp^2/\omega^2 = \epsilon_{yy}$), given by (50), may be written as

$$\frac{c^2k_\perp^2}{\omega^2} = 1 - \sum_\alpha \frac{\omega_{p\alpha}^2}{\omega^2} \sum_{n=1}^{\infty} \left(\frac{n^2\Gamma_n(\lambda_\alpha)}{\lambda_\alpha} - 2\lambda_\alpha\, \Gamma_n'(\lambda_\alpha) \right) \times \left(\frac{2\omega^2}{\omega^2 - n^2\Omega_{0\alpha}^2} \right) + 2\sum_\alpha \frac{\omega_{p\alpha}^2}{\omega^2} \lambda_\alpha\, \Gamma_0'(\lambda_\alpha) \qquad (53)$$

The two X-mode dispersion relations, (52) and (53), contain the standard modified Bessel function. We can solve these relations numerically to describe the X-mode in detail. Alternatively, we can seek an approximate analytical solution results by expanding the Bessel function for small argument, which converts (52), and (53) to the form

$$\frac{c^2k_\perp^2}{\omega^2} = \left\{ 1 - \sum_\alpha \frac{\omega_{p\alpha}^2}{\omega^2} \sum_{n=1}^{\infty} \frac{n^2}{n!} \left(\frac{k_\perp v_{t\perp}}{2\Omega_{0\alpha}} \right)^{2n-2} \left(\frac{\omega^2}{\omega^2 - n^2\Omega_{0\alpha}^2} \right) \right\} - \left[\frac{\left\{ \sum_\alpha \frac{\omega_{p\alpha}^2}{\omega^2} \sum_{n=1}^{\infty} \frac{n^2}{n!} \left(\frac{k_\perp v_{t\perp}}{2\Omega_{0\alpha}} \right)^{2n-2} \left(\frac{n\omega\Omega_{0\alpha}}{\omega^2 - n^2\Omega_{0\alpha}^2} \right) \right\}^2}{\left\{ 1 - \sum_\alpha \frac{\omega_{p\alpha}^2}{\omega^2} \sum_{n=1}^{\infty} \frac{n^2}{n!} \left(\frac{k_\perp v_{t\perp}}{2\Omega_{0\alpha}} \right)^{2n-2} \left(\frac{\omega^2}{\omega^2 - n^2\Omega_{0\alpha}^2} \right) \right\}} \right], \qquad (54)$$

and

$$\frac{c^2k_\perp^2}{\omega^2} = 1 - \sum_\alpha \frac{\omega_{p\alpha}^2}{\omega^2} \sum_{n=1}^{\infty} \frac{n^2}{n!} \left(\frac{k_\perp v_{t\perp}}{2\Omega_{0\alpha}} \right)^{2n-2} \left(\frac{\omega^2}{\omega^2 - n^2\Omega_{0\alpha}^2} \right), \qquad (55)$$

respectively.

Equation (55) is the expression derived by Zaheer and Murtaza for pure transverse X-modes [73]. Equation (54) with the sums over n on the right-hand side truncated at $n = 1$ reduces to the textbook expression for the dispersion relation for the general X-mode in electron plasmas (see, e. g., Chen [1]):

$$\frac{c^2k_\perp^2}{\omega^2} = 1 - \frac{\omega_{pe}^2}{\omega^2} \left(\frac{\omega^2 - \omega_{pe}^2}{\omega^2 - (\omega_{pe}^2 + \Omega_{0e}^2)} \right) \qquad (56)$$

Bernstein Wave In view of the expression for ϵ_{xx}, (43), the dispersion relation for the Bernstein wave $\epsilon_{xx} = 0$ in (51) takes the form

$$1 = 2\sum_\alpha \frac{\omega_{p\alpha}^2}{\omega^2} \left(\frac{\exp[-\lambda_\alpha]}{\lambda_\alpha} \right) \sum_{n=1}^{\infty} n^2 I_n(\lambda_\alpha) \left(\frac{\omega^2}{\omega^2 - n^2\Omega_{0\alpha}^2} \right), \qquad (57)$$

Figure 7 depicts solutions of this equation. The dotted line represents the solution for $\lambda_e = 1$ and the other three curves represent $\lambda_e = 0.5$, 1.5, and 2.0. The resonance points are fixed, but the cutoff points shift from right to left and reduce the propagation domain as λ_e grows. At higher harmonics (not shown), the cutoff points become independent of λ_e.

O-Mode Given the expression for ϵ_{zz} (45) the dispersion relation for the O-mode in (49) is given by the equality

$$\frac{c^2k_\perp^2}{\omega^2} = 1 - \sum_\alpha \frac{\omega_{p\alpha}^2}{\omega^2} \Gamma_0(\lambda_\alpha) - 2\sum_\alpha \frac{\omega_{p\alpha}^2}{\omega^2} \sum_{n=1}^{\infty} \Gamma_n(\lambda_\alpha) \times \left\{ 1 + \frac{T_{\parallel\alpha}}{T_{\perp\alpha}} \frac{n^2\Omega_{0\alpha}^2}{\omega^2 - n^2\Omega_{0\alpha}^2} \right\} \qquad (58)$$

Again we expand the Bessel function for small argument and rewrite this equation in the form

$$\frac{c^2k_\perp^2}{\omega^2} = 1 - \sum_\alpha \frac{\omega_{p\alpha}^2}{\omega^2} - 2\sum_\alpha \frac{\omega_{p\alpha}^2}{\omega^2} \sum_{n=1}^{\infty} \frac{1}{n!} \left(\frac{k_\perp v_{t\perp}}{2\Omega_{0\alpha}} \right)^{2n} \times \left\{ \frac{\omega^2}{\omega^2 - n^2\Omega_{0\alpha}^2} - \left(1 - \frac{T_{\parallel\alpha}}{T_{\perp\alpha}} \right) \frac{n^2\Omega^2}{\omega^2 - n^2\Omega_{0\alpha}^2} \right\} \qquad (59)$$

This is a general dispersion relation for the O-mode with higher order thermal effects, including the consequences of thermal anisotropy.

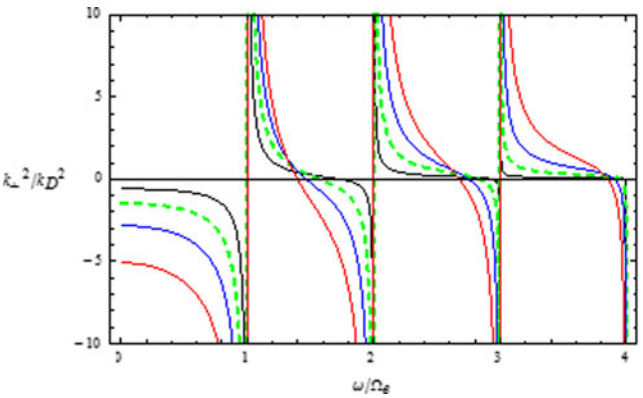

Fig. 7 (*Color online*) Graphical depiction of the Bernstein model. The dotted line represents the solution for $\lambda_e = 1$ and the other three curves represent $\lambda_e = 0.5$ (*black*), 1.0 (*green*), 1.5 (*blue*), and 2.0 (*red*). The resonance points are fixed, but the cutoff points shift from *right* to *left* and reduce the propagation domain as λ_e grows. At higher harmonics (not shown), the cutoff points become independent of λ_e

2.2.3 Oblique Propagation

In the low-frequency, long parallel-wavelength regime, the non-diagonal components of the tensor ε_{ij} are negligibly small. Therefore the dispersion relation in (9), for the kinetic Alfvén waves (KAWs) can be written as

$$\begin{vmatrix} \varepsilon_{xx} - N_{\parallel}^2 & N_{\parallel} N_{\perp} \\ N_{\parallel} N_{\perp} & \varepsilon_{zz} - N_{\perp}^2 \end{vmatrix} = 0. \tag{60}$$

In this regime, the fast mode is described by the expression

$$\varepsilon_{yy} - N^2 = 0, \tag{61}$$

and is hence decoupled from the KAWs.

The electric field vector **E** and the wavenumber vector **k** are coplanar for the KAWs [68–70].

Reference [52] presents a detailed derivation of the expressions describing the oblique propagation of the KAWs in the kinetic and inertial limits. Here we present a simpler derivation. To highlight the effects of thermal anisotropy and to show the wave frequency ω as a function of the perpendicular and parallel wave vectors $k_{\parallel}$ and $k_{\perp}$, we present a 3-D graphical representation of the simplified results. To the best of our knowledge, our results for the general fast mode and the fast mode instability are new.

General expressions for the components of the tensor ε_{ij} were presented in Section 2.1. We substitute (10) for ε_{xx} and (12) for ε_{zz} and consider the low-frequency limit $\omega \ll \Omega_i$, $k_{\parallel}^2 \lambda_{De}^2 \ll 1$, $V_A^2 \ll c^2$ to reduce (60) to the equality

$$\left(\frac{\omega^2}{k_{\parallel}^2 V_A^2} - \frac{(1+\psi_1)\lambda_i}{1-\Gamma_0(\lambda_i)} \right) \times \left(-\frac{\Gamma_0(\lambda_e)}{2k_{\parallel}^2 \lambda_{De}^2} Z'(\xi_{0e}) - \frac{\Gamma_0(\lambda_i)}{2k_{\parallel}^2 \lambda_{Di}^2} Z'(\xi_{0i}) + \frac{\omega_{pi}^2}{\omega^2} \psi_2 \right) = \left(\frac{\omega^2}{k_{\parallel}^2 V_A^2} - \left(\frac{\lambda_i}{1-\Gamma_0(\lambda_i)} \right) \psi_1 \right) \frac{c^2 k_{\perp}^2}{\omega^2} \tag{62}$$

with the shorthand

$$\lambda_{D\alpha}^2 = \frac{v_{t\parallel\alpha}^2}{2\omega_{p\alpha}^2}.$$

Here, the anisotropy terms ψ_1 and ψ_2 are

$$\psi_1 = \frac{c_{s_{\parallel}}^2}{V_A^2} \left\{ \left(\frac{1-\Gamma_0(\lambda_i)}{\lambda_i} \right) \left(\frac{T_{\perp i}}{T_{\parallel i}} - 1 \right) \left(\frac{T_{\parallel i}}{T_{\parallel e}} \right) + \left(\frac{1-\Gamma_0(\lambda_e)}{\lambda_e} \right) \left(\frac{T_{\perp e}}{T_{\parallel e}} - 1 \right) \right\}, \tag{63}$$

and

$$\psi_2 = \left\{ \frac{m_i}{m_e} (1-\Gamma_0(\lambda_e)) \left(\frac{T_{\parallel e}}{T_{\perp e}} - 1 \right) + (1-\Gamma_0(\lambda_i)) \times \left(\frac{T_{\parallel i}}{T_{\perp i}} - 1 \right) \right\} \tag{64}$$

Although in (62), we have included contributions from both species for terms containing anisotropic effect but we have neglected the electronic contribution from the isotropic part of the ϵ_{xx} component by using the small mass ratio, $m_e/m_i \ll 1$.

Next, we shall derive the dispersion relation for the kinetic Alfvén wave in the kinetic (i.e., $v_{t\parallel i} \ll \omega/k_{\parallel} \ll v_{t\parallel e}$ and $(m_e/m_i) \ll \beta = (c_{s_{\parallel}}^2/V_A^2) \ll 1$) and in the inertial ($v_{t\parallel e,i} \ll \omega/k_{\parallel}$, $\beta \ll m_e/m_i$) limits. The kinetic (inertial) limit is defined with reference to the dominant thermal (inertial) electronic effect.

KAWs in the Kinetic Limit To discuss the kinetic limit of KAWs, we assume the parallel phase velocity of the wave to be less than the parallel thermal velocity of the electrons, yet greater than the parallel thermal velocity of the ions, i.e., $v_{t\parallel i} \ll \omega/k_{\parallel} \ll v_{t\parallel e}$, and the plasma to have low β, i.e., $(m_e/m_i) \ll \beta = (c_{s_{\parallel}}^2)/V_A^2) \ll 1$. Under these conditions, the dispersion relation in (62) reduces to

$$\omega^2 = k_{\parallel}^2 V_A^2 \left\{ 1 + \frac{3}{4} k_{\perp}^2 \rho_i^2 + k_{\perp}^2 \rho_s^2 + \psi_1' \frac{c_{s_{\parallel}}^2}{V_A^2} \right\}, \tag{65}$$

where

$$\psi_1' = \left\{ \left(1 - \frac{3}{4} k_{\perp}^2 \rho_e^2 \right) \left(\frac{T_{\perp e}}{T_{\parallel e}} - 1 \right) + \frac{T_{\parallel i}}{T_{\parallel e}} \left(1 - \frac{3}{4} k_{\perp}^2 \rho_i^2 \right) \times \left(\frac{T_{\perp i}}{T_{\parallel i}} - 1 \right) \right\}, \tag{66}$$

and

$$\rho_s^2 = \frac{c_{s_{\parallel}}^2}{\Omega_{0i}^2}$$

In deriving (65) we have assumed the gyro-radii to be small, so that

$$\Gamma_0(\lambda_{e,i}) \approx 1 - \lambda_{e,i} + \frac{3}{4}\lambda_{e,i}^2 \quad \text{and} \quad \frac{\lambda_{e,i}}{1-\Gamma_0(\lambda_{e,i})} = \frac{1}{1 - \frac{3}{4} k_{\perp}^2 \rho_{e,i}^2} \simeq 1 + \frac{3}{4} k_{\perp}^2 \rho_{e,i}^2. \tag{67}$$

Equation (62) describes the general kinetic Alfvén wave, in which ψ_1' measures the deviation from the isotropic limit. Illustrative plots are presented in Fig. 8.

KAWs in the Inertial Limit To obtain the inertial limit of KAWs, we assume that the parallel phase velocity of the wave is greater than the parallel thermal velocities of both the electrons and the ions, i.e., $v_{t\|e,i} \ll \omega/k_\|$, $\beta \ll (m_e/m_i)$, and that the gyroradii are small. Under these constraints, the dispersion relation in (62) yields the following expression for the modified kinetic Alfvén wave in the inertial regime:

$$\omega^2 = k_\|^2 V_A^2 \times \left[\frac{1}{1+\dfrac{c^2k_\perp^2}{\omega_{pe}^2}} + \beta_\| \left\{\frac{T_{\|i}}{T_{\|e}}\left(\frac{T_{\perp e}}{T_{\|e}}-1\right)+\left(\frac{T_{\perp i}}{T_{\|i}}-1\right)\right\}\right]. \tag{68}$$

The inertial Alfvén wave is modified by the acoustic effect, in turn caused by the thermal anisotropy. Since $\beta \ll m_e/m_i$ only extraordinarily large thermal anisotropies will show appreciable effects.

Fast Mode We take advantage of the low-frequency limit $\omega \ll \Omega_{0\alpha}$ and of the Bessel function identity $2\sum_{n=1}^{\infty}\Gamma_n(\lambda_\alpha) = 1-\Gamma_0(\lambda_\alpha)$ and keep only the leading term ($l=0$) in the sum over l on the right-hand side of (20). The fast mode dispersion relation in (61) (i.e., $\varepsilon_{yy} - N^2 = 0$) then reduces to

$$\frac{c^2k^2}{\omega^2} = 1 + \sum_\alpha \frac{\omega_{p\alpha}^2}{\Omega_\alpha^2}\left(\frac{1-\Gamma_0(\lambda_\alpha)}{\lambda_\alpha} - 4\sum_{n=1}^{\infty}\frac{\lambda_\alpha}{n^2}\Gamma_n'(\lambda_\alpha)\right) \times\left\{1-\left(\frac{T_{\perp\alpha}}{T_{\|\alpha}}-1\right)\left(\frac{k_\|^2 v_{t_{\|\alpha}}^2}{2\omega^2}\right)\right\} + 2\sum_\alpha \frac{\omega_{p\alpha}^2}{\omega^2}\lambda_\alpha\,\Gamma_0'(\lambda_\alpha) \times\left\{1+\left(\frac{T_{\perp\alpha}}{T_{\|\alpha}}-1\right)\left(\frac{k_\|^2 v_{t_{\|\alpha}}^2}{2\omega^2}\right)\right\}. \tag{69}$$

Here we have expanded the plasma dispersion function $Z(\xi_{0\alpha})$ for $|\xi_{0\alpha}| \gg 1$.

To further simplify (69), we let $V_A^2 \ll c^2$ and take the small gyro radius limit (in which the argument of the Bessel function is small), so that the term containing $\Gamma_n'(\lambda_\alpha)$ becomes negligible. This leads to the result

$$\frac{c^2k^2}{\omega^2} = 1 + \sum_\alpha \frac{\omega_{p\alpha}^2}{\Omega_{0\alpha}^2} - \sum_\alpha \frac{\omega_{p\alpha}^2}{\Omega_{0\alpha}^2}\frac{k_\perp^2 v_{\perp\alpha}^2}{\omega^2} - \sum_\alpha \frac{\omega_{p\alpha}^2}{\Omega_{0\alpha}^2}\left(\frac{T_{\perp\alpha}}{T_{\|\alpha}}-1\right)\left(\frac{k_\|^2 v_{t_{\|\alpha}}^2}{2\omega^2}\right), \tag{70}$$

where we have used that $\Gamma_0'(\lambda_\alpha) = -1$ and defined $\rho_\alpha^2 \equiv v_{t\perp\alpha}^2/(2\Omega_{0\alpha})$.

For an electron-ion plasma, this dispersion relation can be written in the form

$$\omega^2 = k^2V_A^2 + k_\perp^2 c_{s_\perp}^2 + k_\|^2 c_{s_\|}^2\left\{\frac{T_{\|i}}{T_{\|e}}\left(\frac{T_{\perp i}}{T_{\|i}}-1\right)+\left(\frac{T_{\perp e}}{T_{\|e}}-1\right)\right\} \tag{71}$$

where

$$\frac{\omega_{pi}^2}{\Omega_i^2} = \frac{c^2}{V_A^2}, \quad c_{s_\perp}^2 = \frac{T_{\perp e}+T_{\perp i}}{m_i}, \quad \text{and} \quad c_{s_\|}^2 = \frac{T_{\|e}}{m_i}.$$

Equation (71), the modified dispersion relation for the fast mode, incorporates the thermal anisotropy effects of the two species. The parallel-propagating term displays an acoustic effect associated with the parallel temperature, i.e., $c_{s_\|}^2$ which is sensitive to the thermal anisotropy. By contrast, the acoustic effect $c_{s_\perp}^2$ associated with the perpendicular-propagating term depends on the perpendicular temperature, but receives no contribution from the temperature anisotropy. In oblique propagation, the general fast mode has therefore two distinct acoustic effects, one in the parallel and the other in the perpendicular direction. The enhancement or the reduction of the fast mode frequency

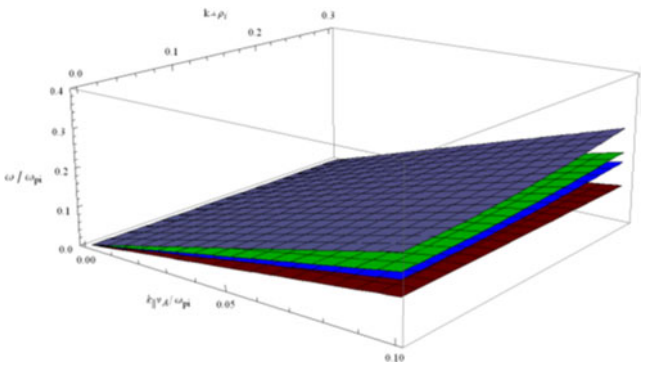

Fig. 8 (*Color online*) Normalized frequency of KAWs in kinetic limit $\omega(k_\|, k_\perp)/\omega_{pi}$ as a function of perpendicular and parallel normalized wavenumber (i.e., $k_\perp\rho_i/\omega_{pi}$ and $k_\| v_A/\omega_{pi}$), $\beta_\| = 0.05$ & $A_e = A_i = A = \left(T_\perp/T_\|\right) - 1$ by choosing different values of thermal anisotropy (i.e., from bottom to top, A=0 (*red*), 10 (*blue*), 20 (*green*), 40 (*purple*)). The frequency increases with the increase of temperature anisotropy value and the effect of temperature anisotropy is more prominent in high beta plasma environments than the low beta one where $T_{\perp\alpha} > T_{\|\alpha}$

depends upon the strength and signature of the thermal anisotropies of the two species.

Figure 9 represents the general fast mode for small and for large $\beta_\parallel$'s. The anisotropy effect becomes more prominent when $\beta_\parallel$ is large.

Three instances of the general fast-mode dispersion relation (71) deserve special mention:

(i) For parallel propagation (i.e., $k_\perp = 0$), (71) gives the Alfvén-wave dispersion relation in (39), namely,

$$\omega^2 = k_\parallel^2 V_A^2 \left[1 + \frac{\beta_\parallel}{2}\left\{\left(\frac{T_{\perp i}}{T_\parallel} - 1\right) + \left(\frac{T_{\perp e}}{T_\parallel} - 1\right)\right\}\right]. \tag{72}$$

Here we have assumed that the two species have the same parallel temperature.

(ii) For perpendicular propagation ($k_\parallel = 0$), (71) yields the standard dispersion relation for the magneto-sonic mode,

$$\omega^2 = k_\perp^2 \left\{V_A^2 + c_{s_\perp}^2\right\}.$$

(iii) In the isotropic limit i.e., $T_{\perp\alpha} = T_{\parallel\alpha} = T_\alpha$ (71) reduces to the standard fast mode dispersion relation

$$\omega^2 = k^2 V_A^2 + k_\perp^2 c_s^2,$$

where

$$c_s^2 = \frac{T_e + T_i}{m_i}$$

Fast Mode Instability Under the constraint

$$\frac{\left(1 + \frac{c_{s_\perp}^2}{V_A^2}\right)}{\left[\frac{c_{s_\parallel}^2}{V_A^2}\left\{\frac{T_{\parallel i}}{T_{\parallel e}}\left(1 - \frac{T_{\perp i}}{T_{\parallel i}}\right) + \left(1 - \frac{T_{\perp e}}{T_{\parallel e}}\right)\right\} - 1\right]} < \frac{k_\parallel^2}{k_\perp^2}, \tag{73}$$

the fast mode, (71), becomes unstable, since

$$\omega = i\left[k_\parallel^2 V_A^2\left[\frac{c_{s_\parallel}^2}{V_A^2}\left\{\frac{T_{\parallel i}}{T_{\parallel e}}\left(1 - \frac{T_{\perp i}}{T_{\parallel i}}\right) + \left(1 - \frac{T_{\perp e}}{T_{\parallel e}}\right)\right\} - 1\right] - k_\perp^2 V_A^2\left(1 + \frac{c_{s_\perp}^2}{V_A^2}\right)\right]^{\frac{1}{2}}. \tag{74}$$

The inequality (73) requires that $\beta_\parallel = c_{s_\parallel}^2 / V_A^2 \gg 1$ and that $T_{\perp\alpha} < T_{\parallel\alpha}$.

In (74), the parallel-propagating part represents the Alfvén wave with thermal anisotropy while the perpendicular part represents the magneto-sonic wave, which tends to suppress instabilities. Therefore, fire-hose instabilities may be damped for small perpendicular wavelengths, as demonstrated by Fig. 10.

In the other limit, $|\xi_{n\alpha}| \leq 1$, we expand the plasma dispersion function as

$$Z(\xi_{n\alpha}) = i\sqrt{\pi} - 2\xi_{n\alpha}\left(1 - \frac{2\xi_{n\alpha}^2}{3} + \frac{4\xi_{na}^4}{15} + \ldots.\right) = i\sqrt{\pi} + \sum_{l=0}^{\infty} \frac{(-2)^{l+1}}{(2l+1)!!}\left(\frac{\omega - n\Omega_\alpha}{k_\parallel v_{t\parallel\alpha}}\right)^{2l+1}, \tag{75}$$

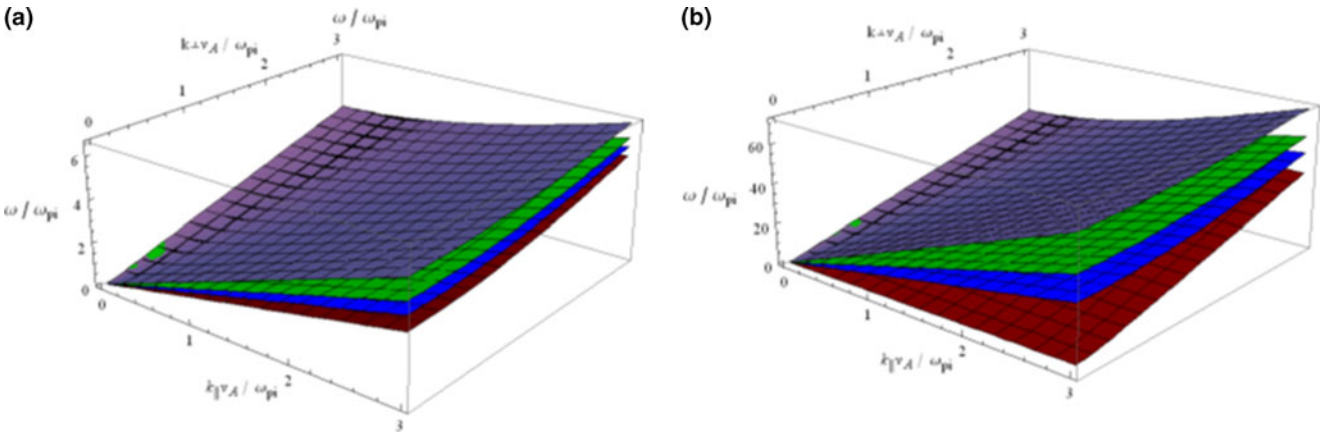

Fig. 9 (*Color online*) Normalized fast mode frequency $\omega\left(k_\parallel, k_\perp\right)/\omega_{pi}$ as a funtion of perpendicular and parallel normalized wavenumber i.e., ($k_\parallel v_A/\ \omega_{pi}$ & $k_\perp v_A/\omega_{pi}$) with the parameters $A_e = A_i = A = \left(T_\perp/T_\parallel\right) - 1$; (**a**) $\beta_\parallel = 0.05$ & (**b**) $\beta_\parallel = 10.0$ by choosing different values of thermal anisotropy (i.e., from bottom to top, A=0 (*red*), 10 (*blue*), 15 (*green*), 30 (*purple*). The frequency increases with the increase of temperature anisotropy value and the effect of temperature anisotropy is more prominent in high beta plasma environments than the low beta one where $T_{\perp\alpha} > T_{\parallel\alpha}$

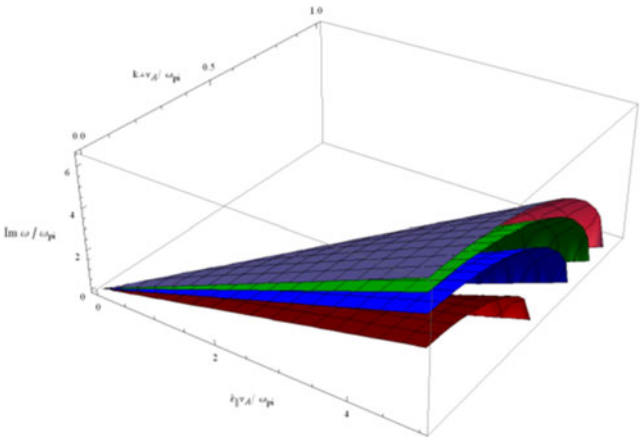

Fig. 10 (*Color online*) Normalized growth rate Im $\omega\left(k_{\parallel}, k_{\perp}\right)/\omega_{pi}$ of fast mode instability as a function of perpendicular and parallel normalized wavenumber i.e., ($k_{\parallel}v_A/\ \omega_{pi}$ & $k_{\perp}v_A/\omega_{pi}$) with the parameters $A_e = A_i = A = \left(T_{\parallel}/T_{\perp}\right)$ & $\beta_{\parallel} = 3.0$ by choosing different values of thermal anisotropy (i.e., from bottom to top, A=0 (*red*), 2 (*blue*), 4 (*green*), 9 (*purple*)). The growth rate enhances with the increase of temperature anisotropy but the perpendicular wave vector stabilizes this instability i.e., the magneto-sonic wave suppresses the fire-hose instability which exist only in the high beta plasma environment where with $T_{\perp\alpha} > T_{\parallel\alpha}$

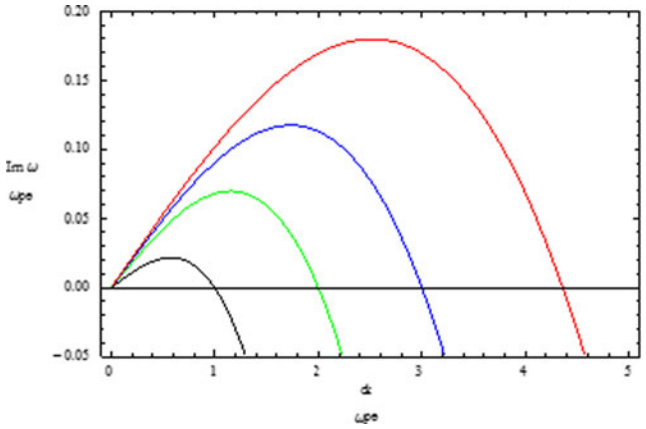

Fig. 11 (*Color online*) Normalized growth rate Im ω/ω_{pe} of non-resonant whistler instability ($|\xi_{n\alpha}| \leq 1$) as a function of normalized wavenumber ck/ω_{pe} with the parameters $v_{t\parallel}/c = 0.1$ & $A = \left(T_{\perp e}/T_{\parallel e}\right) - 1$ by choosing different values of thermal anisotropy, i.e., from left to right, A=0 (*black*), 5 (*green*), 10 (*red*), 20 (*blue*). By increasing the temperature anisotropy, The growth rate increases and threshold on wave number shifts towards the longer wavelength and thus enlarges the wave vector domain. This instability exist only in the plasma environment where with $T_{\perp\alpha} > T_{\parallel\alpha}$

and proceed to discuss the parallel-propagating whistler instability.

Resonant Whistler Instability ($|\xi_{n\alpha}| \leq 1$) With (10), (11), and (13), the dispersion relation for R-waves in electron plasma becomes

$$\frac{c^2k_{\parallel}^2}{\omega^2} = 1 + \frac{\omega_{pe}^2}{\omega^2}\left[\left(\frac{T_{\perp e}}{T_{\parallel e}} - 1\right) + i\sqrt{\pi}\frac{\omega}{k_{\parallel}v_{t_{\parallel e}}} \times \left\{\frac{T_{\perp e}}{T_{\parallel e}} - \frac{\Omega_{oe}}{\omega}\left(\frac{T_{\perp e}}{T_{\parallel e}} - 1\right)\right\}\right], \tag{76}$$

where we have kept only the leading term of the plasma dispersion function for $|\xi_{n\alpha}| \leq 1$.

Under the subluminal condition, i.e., for $\omega \ll ck$, the real and imaginary parts of ω are

$$\Re\omega = \Omega_{0e}\left(1 - \frac{T_{\parallel e}}{T_{\perp e}}\right), \tag{77}$$

and

$$\Im\,\omega = \frac{k_{\parallel}v_{t_{\parallel e}}}{\sqrt{\pi}}\left(\frac{T_{\parallel e}}{T_{\perp e}}\right)\left[\left(\frac{T_{\perp e}}{T_{\parallel e}} - 1\right) - \frac{c^2k_{\parallel}^2}{\omega_{pe}^2}\right]. \tag{78}$$

This defines the whistler instability, which occurs for waves satisfying the wavenumber condition

$$k_{\parallel}^2 < \frac{\omega_{pe}^2}{c^2}\left(\frac{T_{\perp e}}{T_{\parallel e}} - 1\right).$$

The magnetic field generates real oscillations, but the growth rate remains unaffected. These results coincide with those due to Lazar et al. [42]. Figure 11 exhibits the effect of anisotropy on the whistler instability. For the field-free case, i.e., $B_0 = 0$, only the purely growing Weibel instability arises [25].

3 Summary of Results and Discussion

On the basis of kinetic theory, we have extensively reviewed plasma waves and instabilities. In particular, we find that for any anisotropic equilibrium distribution, here included the non-relativistic, relativistic, and ultra-relativistic magnetized collisionless homogeneous plasmas, the electrostatic modes are insensitive to thermal anisotropies, which affect only the electromagnetic modes with magnetic field perturbations perpendicular to the ambient magnetic field.

We have also derived expressions describing a general dielectric tensor for a magnetized non-relativistic bi-Maxwellian plasma. In alignment with the salient physical features of the problem, our analysis showed that the dielectric tensor receives separate contributions from the integrations over the perpendicular and the parallel momentum components. The integration over the perpendicular components leads to the functions $\Gamma_n(\lambda_\alpha)$ and $\Gamma_n'(\lambda_\alpha)$, which are related to the modified Bessel function $I_n(\lambda_\alpha)$, while the integration

over the parallel components introduces the plasma dispersion functions $Z(\xi_{n\alpha})$ and $Z'(\xi_{n\alpha})$. From the resulting general dielectric tensor we have obtained the dispersion relations for a variety of modes and instabilities.

We have also expanded the plasma dispersion functions in the limit $|\xi_{n\alpha}| \gg 1$ to derive relatively simple analytical expressions for the components of dielectric tensor and to find the dispersion relations for those modes and instabilities. For example, (i) for parallel propagation, we have expanded the modified Bessel function as $k_\perp \to 0$ and note that only $n = 1$ terms survive. We have also derived the dispersion relations for the R- and L- waves, whistler wave, Alfvén wave, Langmuir wave, non-resonant whistler instability, Weibel instability and Alfvén-wave instability; (ii) for perpendicular propagation, we have let $k_\parallel \to 0$ and noted that only the leading term ($l = 0$) in the sum over l survives to derive the general dispersion relations for the X-, O-, and Bernstein modes. (iii) For oblique propagation, we have found the general dispersion relations for the kinetic Alfvén wave in the kinetic and the inertial regimes and for the fast mode. Additionally, we have discussed a few special cases of the fast mode and the fast mode instability. For $|\xi_{n\alpha}| \leq 1$, we have derived the parallel-propagating whistler instability.

In both limiting cases, as expected, the electrostatic modes are unaffected by the thermal anisotropy. Among the electromagnetic modes, the parallel-propagating modes, such as the R- and L- waves and the modes derived from them (the whistler mode, pure Alfvén mode, firehose instability, and Weibel instability) are affected, while the perpendicularly-propagating modes, such as the X-mode and the modes derived from it (the pure transverse X- and Bernstein modes) are not. The O-mode, however, is sensitive to thermal anisotropies.

The thermal anisotropy affects the parallel propagating modes via the acoustic effect, while it affects the perpendicular propagating modes via Larmor-radius effects. For oblique propagation, both effects appear, additively, in the Alfvénic modes.

The effects of thermal anisotropies are more prominent in the kinetic limit than the inertial limit. The parallel-propagating term of the fast mode displays an acoustic effect with parallel temperature, i.e., $c_{s_\parallel}^2$ controlled by the thermal anisotropy. On the other hand, the perpendicular-propagating term displays an acoustic effect with perpendicular temperature, i.e., $c_{s_\perp}^2$, but it is independent of the thermal anisotropy. In oblique propagation, the general fast mode presents two distinct acoustic effects, in the parallel and perpendicular directions.

For both the resonant and the non-resonant cases, the whistler and Weibel instabilities can only exist in environments with $T_{\perp\alpha} > T_{\parallel\alpha}$ whereas the firehose and the general fast-mode instabilities can only arise for $T_{\parallel\alpha} > T_{\perp\alpha}$.

In conclusion, we find that the thermal anisotropy affects only the modes with magnetic perturbations perpendicular to the ambient magnetic field i.e., with $\mathbf{B}_1 \perp \mathbf{B}_0$. The anisotropy can either enhance or reduce the frequency domain of waves and instabilities, depending on its strength and signature.

Our results may prove useful for studies of the thermally anisotropic environments frequently found in astrophysical, space, and even laboratory plasmas.

Acknowledgements We are thankful to the anonymous Referee for making several useful suggestions to improve the quality of this review paper and to the Office of the External Activities of the ICTP, Trieste, Italy, for providing partial financial support to Salam Chair, at GC University Lahore.

References

1. F.F. Chen, *Introduction to Plasma Physics and Controlled Fusion*, vol. 1 (Plenum Press, New York, 1984)
2. S. Ichimaru, *Basic Principles of Plasma Physics* (Addison-Wesley Press, Tokyo, 1973)
3. M. Brambilla, *Kinetic Theory of Plasma Waves Homogeneoues plasmas* (Oxford University Press, New York, 1998)
4. R. Gaelzer, L.F. Ziebell, R.S. Schneider., Braz. J. Phys. **34**, 1224 (2004)
5. L.F. Ziebell, R.S. Schneider, Braz. J. Phys. **34**, 1211 (2004)
6. M. Miyamoto, *Plasma Physics for Nuclear Fusion* (MIT Press, New York, 1980)
7. A.F. Alexandrov, L.S. Bogdankevich, A.A. Rukhadze, *Principles of Plasma Electrodynamics* (Springer-Verlag Berlin Heidelberg Press, New York, 1984)
8. D.C. Montgomery, D.A. Tidman, *Plasma Kinetic Theory* (McGraw-Hill Press, New York, 1964)
9. R.L. Mace, Phys. Scr. **T63**, 207 (1996)
10. A. Bret, M.C. Firpo, C. Deutsch, Phys. Rev. E. **70**, 046401 (2004)
11. M.W. Verdon, D.B. Melrose, Phys. Rev. E. **77**, 046403 (2008)
12. G. Noci, J.L. Kohl, G.L. Withbroe, ApJ. **315**, 706 (1987)
13. M. Pagel, Q.D. Atkinson, A. Meade, Nature **449**, 717 (2007)
14. R.W. Schunk, D.S. Watkins, J. Geophys. Res. **86**, 91 (1981)
15. W. Masood, S.J. Schwartz, J. Geophys. Res. **113**, A01216 (2008)
16. C. Cremaschini, J.C. Miller, M. Tessarotto, Phys. Plasmas **17**, 072902 (2010)
17. S.S.A. Gillani, N.L. Tsintsadze, H.A. Shah, M. Razzaq, Phys. Plasmas **17**, 083103 (2010)
18. A. Bret, C. Deutsch, Phys. Plasmas **13**, 022110 (2006)
19. A. Sid, A. Ghezal, A. Soudani, M. Bekhouche, Plasma Fusion Res. **5**, 007 (2010)
20. R.P. Singhal, A.K. Tripathi, Ann. Geophys. **24**, 1705 (2006)
21. E.A. MacDonald, M.H. Denton, M.F. Thomson, S.P. Gary, J. Atmos. Sol.-terr. Phys. **70**, 1789 (2008)
22. F. Xiao, Q. Zhou, H. He, L. Tang, Plasma Phys. Control. Fusion **48**, 1437 (2006)

23. P. Kumar, V.K. Tripathi, Phys. Plasmas **15**, 052107 (2008)
24. R.L. Stenzel, J.M. Urrutia, K.D. Strohmaier, Plasma Phys. Control. Fusion. **50**, 074009 (2008)
25. E.S. Weibel, Phys. Rev. Lett. **2**, 83 (1959)
26. P.H. Yoon, Phys. Fluids B. **1**, 1336 (1989)
27. P.H. Yoon, Phys. Plasmas **14**, 024504 (2007)
28. Y. Sentoku, K. Mima, Z.M. Sheng, P. Kaw, K. Nishihara, K. Nishikawa, Phys. Rev. E. **65**, 046408 (2002)
29. S. Zaheer, G. Murtaza, Phys. Plasmas **14**, 022108 (2007)
30. S. Zaheer, G. Murtaza, Phys. Plasmas **14**, 072106 (2007)
31. A. Stockem, M. Lazar, Phys. Plasmas **15**, 014501 (2008)
32. F. Haas, M. Lazar, Phys. Rev. E. **77**, 046404 (2008)
33. C. Thaury, P. Mora, A. Héron, J.C. Adam, T.M. Antonsen, Phys. Rev. E. **82**, 026408 (2010)
34. S. Zaheer and G. Murtaza, Phys. Scr. **81**, (2010)
35. A. Achterberg, J. Wiersma, Astron. Astrophys. **475**, 1 (2007)
36. U. Schaefer-Rolffs, R.C. Tautz, Phys. Plasmas **15**, 062105 (2008)
37. K.H. Lee, Y. Omura, L.C. Lee, C.S. Wu, Phys. Rev. Lett. **103**, 105101 (2009)
38. W. Masood, S.J. Schwartz, J. Geophys. Res. **113**, A01216 (2008)
39. T.B. Yang, Y. Gallant, J. Arons, A.B. Langdon, Phys. Fluids B, **5**, 3369 (1993)
40. R.C. Davidson, I. Kaganovich, E.A. Startsev, H. Qin, M. Dorf, A. Sefkow, D.R. Welch, D.V. Rose, S.M. Lund, Nucl. Instrum. Methods Phys. Res. **A577**, 70 (2007)
41. E.A. Startsev, R.C. Davidson, Phys. Plasmas **10**, 4829 (2003)
42. M. Lazar, R. Schlickeiser, S. Poedts, Phys. Plasmas **16**, 012106 (2009)
43. H. Alfvén, Nature (London) **150**, 405 (1942)
44. L. Ofman, Astrophys. J. **568**, L135 (2002)
45. B. De Pontieu, S.W. McIntosh, M. Carlsson, V.H. Hansteen, T.D. Tarbell, C.J. Schrijver, A.M. Title, R.A. Shine, S. Tsuneta, Y. Katsukawa, K. Ichimoto, Y. Suematsu, T. Shimizu, S. Nagata, Science **318**, 1574 (2007)
46. W.Gekelman, J. Geophys. Res. **104**, 14417 (1999)
47. R. Schlickeiser, M. Lazar, T. Skoda1, Phys. Plasmas **18**, 012103 (2011)
48. P.H. Yoon, Phys. Fluids **B2**, 842 (1990)
49. R. Schlickeiser, T. Skoda, Astrophys. J. **716**, 1596 (2010)
50. M. Lazar, S. Poedts, A. & A. **494**, 311 (2009)
51. A. Hasegawa, C. Uberoi, *The Alfvén Wave. DOE Critical Review Series—Advances in Fusion Science and Engineering* (Technical Information Service, U.S. Department of Energy, Washington, D.C., 1982)
52. M.F. Bashir, Z. Iqbal, I. Aslam, G. Murtaza, Phys. Plasmas **17**, 102112 (2010)
53. L. Chen, D.J. Wu, Phys. Plasmas **17**, 062107 (2010)
54. M.Y. Yu, P.K. Shukla, Phys. Fluids **21**, 1457 (1978)
55. P.M. Bellan, Adv. Space Res **28**, 729 (2001)
56. H. Saleem, S. Mahmood, Phys. Plasmas **10**, 2612 (2003)
57. G. Murtaza, M.Y. Yu, P.K Shukla, Phys. Rev. A. **30**, 1533 (1984)
58. R.L. Lysak, W. Lotko, J. Geophys. Res. **101**, 5085 (1996)
59. R.L. Lysak, M.K. Hudson, Geophys. Res. Lett. **6**, 661 (1979)
60. J.R. Wygant, A. Keiling, C.A. Cattell, R.L. Lysak, M. Temerin, F.S. Mozer, C.A. Kletzing, J.D. Scudder, V. Streltsov, W. Lotko, C.T. Russell, J. Geophys. Res. **107**, 1201 (2002)
61. A. Hirose, A. Ito, S.M. Mahajan, S. Ohsaki, Phys. Lett. A. **330**, 474 (2004)
62. R. Mishra, M.S Tiwari, Planet. Space Sci. **54**, 188 (2006)
63. G. Ahirwar, P. Varma, M.S. Tiwari, Ann. Geophys. **24**, 1919 (2006)
64. G. Ahirwar, P. Varma, M.S. Tiwari, Ann. Geophys. **24**, 557 (2007)
65. S.P. Duan, Z.Y. Li, Z.X. Liu, Planet. Space Sci. **53**, 1167 (2005)
66. K. Zubia, N. Rubab, H.A. Shah, M. Salimullah, G. Murtaza, Phys. Plasmas **14**, 032105 (2007)
67. N. Rubab, N.V. Erkaev, D. Langmayr, H.K. Biernat, Phys. Plasmas **17**, 103704 (2010)
68. N. Shukla, R. Mishra, P. Varma, M.S. Tiwari, Plasma Phys. Control. Fusion **50**, 025001 (2008)
69. M. Salimullah, M. Rosenberg, Phys. Lett. A. **254**, 347 (1999)
70. N. Shukla, P. Varma, M.S. Tiwari, Indian J. Pure Appl. Phys. **47**, 350 (2009)
71. W. Gekelman, S. Vincena, B.V. Compernolle, G.J. Morales, J.E. Maggs, P. Pribyl, T.A. Carter, Phys. Plasmas **18**, 055501 (2011)
72. B.D. Fried, S.D. Conte, *The Plasma Dispersion Function* (Academic Press, New York, 1961)
73. S. Zaheer, G Murtaza, Phys. Scr. **77**, 035503 (2008)